UNIVERSITÀ DEGLI STUDI DI PADOVA

Department of information engineering

Master's degree course in engineering

Master Thesis

CGM based basal-insulin titration in insulin-naïve type 2 diabetic subjects: an in-silico study

Relatrice
Prof.ssa Chiara Dalla Man

Correlatore
Dott. Jacopo Bonet

Laureando: Paolo Pavone
Matricola: 2045646

Anno Accademico 2022/2023

Index

Abstract

The pathophysiology of the type 2 diabetes (T2D) consists in a malfunctioning of the feedback loops between insulin secretion (β-cell disfunction) and/or insulin action (insulin resistance state) leading to an abnormally high blood glucose level. With the progression of the disease (advance stage T2D), subjects may need exogenous insulin to control their glycaemia, using fast acting insulins during meals and/or long-acting insulins, to control fasting (pre-breakfast) and postprandial glucose concentration. The current procedure to determine the optimal basal insulin dose in subjects who have never previously used insulin to treat diabetes (insulin-naïve) consists in a non-personalized titration rule. According to ADA guidelines, subjects must start the titration with a low insulin dose that is progressively adjusted, following predefined increments/decrements, based only on self-monitoring blood glucose (SMBG) pre-breakfast measurements to reach a target fasting glucose level (FPG). The aim of this thesis is to develop a more personalized basal insulin titration rule based on subjects' specific insulin needs, continuous glucose monitoring (CGM) and common CGM metrics used by clinician to assess the quality of glucose control i.e., time above range (TAR), time in range (TIR), and time below range (TBR). We used a dataset consisting of 300 in silico subjects who underwent a literature titration rule (DUAL I). Subjects were then classified as high insulin needs (HIN) and low insulin needs (LIN), based on their final insulin dose, using a literature logistic regression model. The classified HIN subjects underwent four new algorithms and their GCM time metrics were compared with the ones obtained using DUAL I. Among the new tested algorithm, the best one, which is selected in terms of higher correlation with DUAL I final insulin dose (ρ=0.82, p-value<10^{-8}), showed a statistically and clinically significant increase of TIR, as well as a significant decrease of TAR accompanied by a significant reduction in the FPG. The main drawback was a statistically significant increase in the TBR until the third month, anyway after this period this difference was not significant anymore.

Despite the overall good results achieved, improvements could be made in the future, looking if other trends can add significant features which improve the decision process, but also making studies on how to tune the aggressiveness of the algorithms object of this thesis.

CHAPTER 1

INTRODUCTION

Here, the type 2 diabetes (T2D), its epidemiology and pathophysiology are described, with particular focus on β-cell disfunction and insulin resistance state (IR), followed by a representation on the current therapy, i.e. self-monitoring blood glucose (SBMG) and basal insulin titration for the long-acting insulin.
After that, the continuous glucose monitoring (CGM) approach is presented, as part of the minimally invasive (MI) technologies, as a much more effective method for evaluating subjects' glycemic variations.

1.1 Type 2 diabetes

The prevalence of type 2 diabetes (T2D) is globally rising[1]. In 2017 approximately 462 million individuals were affected by type 2 diabetes corresponding to 6.28% of the world's population (4.4% of those aged 15-49 years, 15% of those aged 50-69 years, and 22% of those aged >70 years), or a prevalence rate of 6059 cases per 100.000. The burden is rising at a much faster rate in developed regions, such as Western Europe, and is projected to be 7079 individuals per 100.000 by 2030, reflecting a generalized worldwide rise. However, the incidence and prevalence of T2D varies depending on ethnicity and geographical region. T2D risk factor include a complex combination of genetic, metabolic, and environmental factors that interact with one another[2]. Despite the fact that genetic predisposition plays an important part in the risk of developing T2D, obesity (body-mass index [BMI]$\geq$30 kg/m^2) is the strongest risk factor for T2D[2,3], followed by a sedentary lifestyle[2].
The pathophysiology of the T2D regards a malfunctioning of the feedback loops between insulin action and insulin secretion bringing to an abnormally high glucose level in blood. In figure 1.1, it is reported a schematic version of the consequence of β-cell disfunction, for which insulin secretion is reduced undermining the ability of glucose cell uptake, and insulin resistance (IR) which contributes to an increased glucose production in the liver and decreased glucose uptake in the muscle, liver, and adipose tissues. Even if both processes play a crucial role in the development of the disease β-cell disfunction is usually more severe than IR[2].

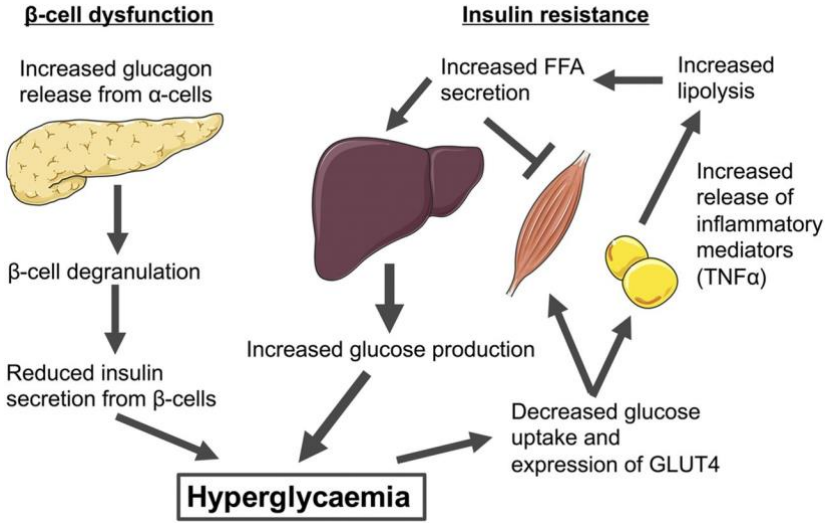

Figure 1.1. Figure from Riddy, D. et.al. Pharmacol. Rev. (2018). Pathophysiolology of T2DM. β-cell dysfunction occurs following an increased FFA levels, obesity, insulin resistance, and inflammation. Initially, the β -cell compensates by increasing the release of insulin; however, over time, this compensatory mechanism fails and reduction in β-cell mass is evident. The loss of β-cell mass occurs from cellular degranulation, resulting in an increase in glucagon secretion from α-cells and a decrease in insulin secretion. The reduced plasma insulin results in an increase in glucose levels. Glucose-sensitive tissues, including skeletal muscle and adipocytes, are unable to accommodate the increased glucose concentration. Increased fat accumulation in adipocytes also leads to an increase in proinflammatory cytokine release and increased lipolysis. A further release of FFAs stimulates the liver to increase glucose production. Persistent glucose release preserves the hyperglycemic environment, leading ultimately to T2DM.[4]

Moreover, In Figure 1.2 an example on how hyperglycemia could lead to cardiovascular disease (CVD) is shown.

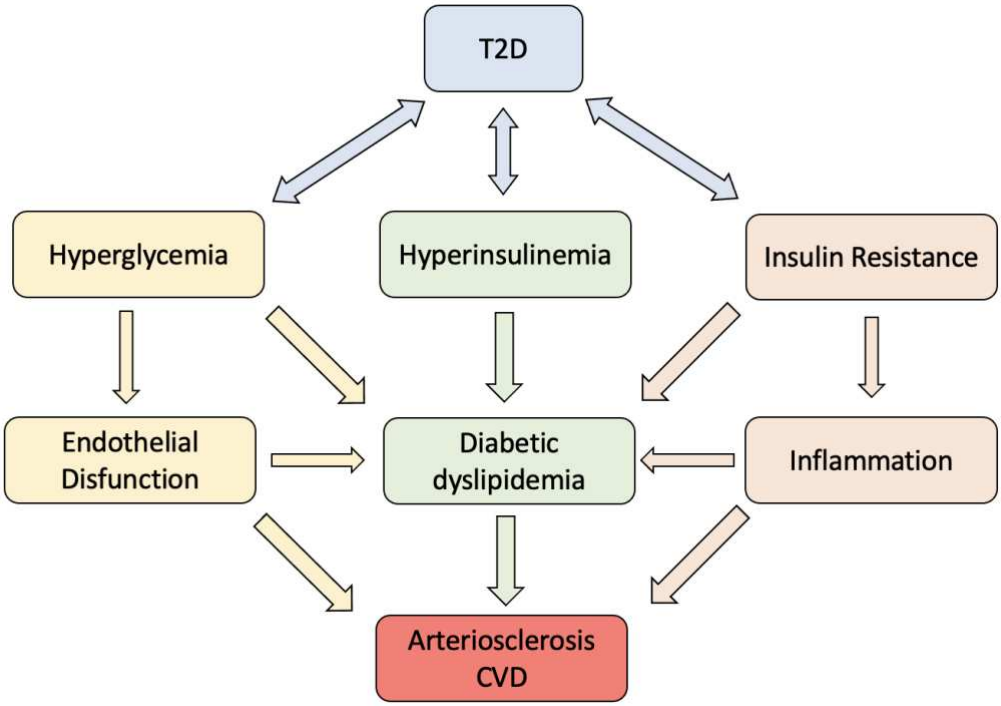

Figure 1.2. Factors implicated in CVD from T2D and the interactions between them. The flowchart illustrates the multiple interactions among the implicated factors[2].

1.2 Current diabetes therapy

The first intervention in T2D subjects is the non-pharmacological therapy, in fact since the accumulation of adipose tissue in the abdominal region is associated to an increased IR, reducing the bodyweight is a powerful method for increasing the insulin sensitivity[5], also coupled with a regular physical activity[6]. Despite the behavioral and diet changes in the majority of the cases the pharmacological treatment is required, and in this field metformin is one of the most used drug, often coupled with exogenous insulin[6]. In particular, T2D subject can use fast-acting and long-acting insulin (mainly distinguished based on how quickly they work, when they peak and how long their action lasts) for rebuilt a proper insulinization and so to reconstruct a physiologic glycemic profile.
Exogenous administered insulin can be characterized by considering the onset, i.e. the time before the insulin enters the bloodstream and starts to lower blood glucose, the peak time i.e. the time at which the lowering blood glucose power is maximum, and the duration i.e. how long insulin continues to lowering glucose concentration.[7]
In particular:

- *Rapid-acting insulins* effects start 15 minutes after injection, peak in about one or two hours after the injection, and last between two to four hours.
- *Regular or short-acting insulins* usually appear in the bloodstream about 30 minutes after the injection, peak from two to three hours after the injection, and their effects last from three to six hours.
- *Long-acting insulins* generally reach the bloodstream several hours after the injection, and lower glucose levels up to 24 hours.
- *Ultra-long acting insulins* reach the bloodstream in six hours, does not peak, and lasts about 36 hours or longer [7].

The administration of fast acting insulin few minutes before the meal determines a more effective suppression of endogenous glucose production, with a reduced raising of the glycemia coupled to a lower risk of late hypoglycemia[8]. Generally, the fast-acting insulin bolus is predetermined based on the meal amount and the target glucose value (Insulin-to- Carb Ratio, CR, and Insulin Correction Factor, CF).
On the other hand, basal insulins are mainly used to maintain pre-breakfast (FPG) and between meals glucose concentration in a target range. However, current procedures to determine the optimal basal insulin dose in subject who have never used insulin before to treat T2D (insulin-naïve) consist in a non-personalized titration rule. In this thesis we always use insulin IDeg to compare the different titration rules developed. Therefore, hereafter a brief description of the Ideg molecule and the standard titration rule (DUAL I) are reported.
Insulin Ideg is an ultra-long acting insulin with an half-life of more than 24 hours and a duration of more than 42 hours[9]. It is fundamental to find a personalized dose of long-acting insulin which brings a rebuilt of the subject basal insulinization[6], thus a better regulation of the hepatic glucose production is achieved during the night and a more effective achievement of fast euglycemia.
In DUALI I trial[10] Ideg insulin was administered and it is proven that it allows a similar control to glargine (another basal insulin) but with lower nocturnal hypoglycemia rates[11]. To determine the optimal basal insulin dose a titration process is needed, working out the right amount of insulin can

often be a difficult task, because the optimal dose, which is not a priori known, depends on a variety of factor. However, for people starting insulin treatment (i.e. insulin-naïve) the American Diabetes Association (ADA) recommends the initiation of basal insulin at 10 U/day which is then adjusted in the following month for matching a specific FPG target [12].

However, the current basal-titration procedure comes with different limitations. First, since it considers just a single value of the daily glycemia (FPG) through self-monitoring blood glucose (SMBG), the titration process typically takes up to one year for providing the final basal-insulin dose to the patient, without considering the glucose time course during the rest of the day. Furthermore, during the titration process the dose administered to the patient is not necessarily the optimal one, hence, the subject is exposed to hyper- and/or hypoglycemia, which in general could lead to a different set of related complications[2].Last, in DUAL I the dose is adapted by increasing/reducing it weekly or twice per week based on predetermined values (more details are provided in Section 2.5.1).

1.3 Minimally invasive glucose measurements

Several techniques to measure glucose concentration are reported in Figure (1.3). Among these, self-monitoring blood glucose (SMBG) are based on a finger-prick test. Its effectiveness depends on different factors, additionally it is not a continuous monitoring process and it requires multiple testing to correct manage meals or physical exercise. Moreover, a non-continuous approach can miss periods of hyper- or hypoglycemia[13]. A possible solution to the above-mentioned problems comes from wearable biosensors, which have the potential to provide continuous, real-time physiological information provided by dynamic, noninvasive measurement of biochemical markers in biofluids. Starting from the 1980s scientist developed new classes of glucose sensors known as enzyme-free or third and fourth generation glucose sensors[14]. Continuous techniques for glucose monitoring belong to fifth generation glucose sensors.

Part of this process are minimally invasive (MI) technologies which rely on the extraction of different fluid from the body (i.e., tears, saliva, sweat and interstitial fluid) to measure glucose concentration through an enzymatic approach that correlate with BG, which is evaluated directly by invasive monitoring[15]. Continuous glucose monitoring (CGM) is an integral part of MI technologies and hence of wearable sensors, despite its usage in real clinical practice remains relatively low[16], CGM metrics can be extracted. They provide more complete information on the glycemia status of the subject to the respect of the SMBG.

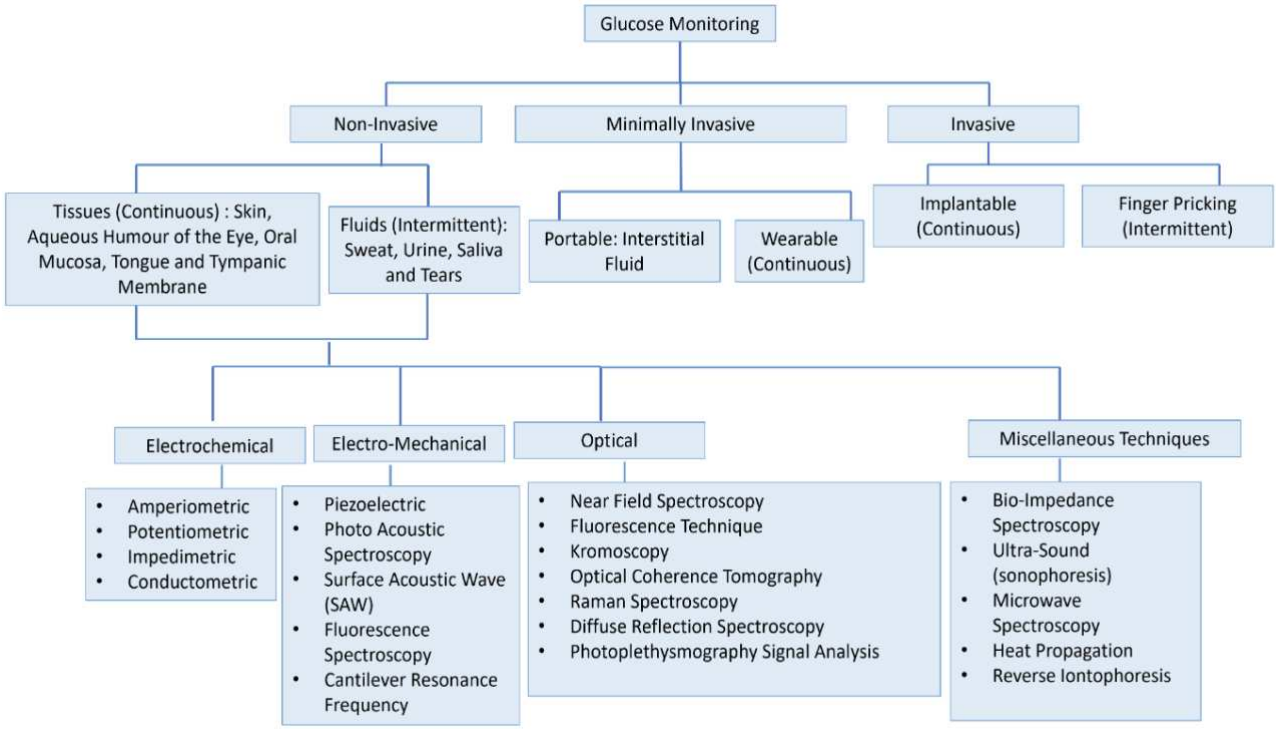

Figure 1.3. Overview of the numerous approaches for measuring glucose[17].

Despite SMBG may help T2D subjects which are treated with insulin, an important role is played by the CGM, which can be used for assessing the safety and also the inter-variability in the therapy response, especially for those on intensive insulin regimens[18].
Overall, it is clear that CGM could lead to significant clinical benefits[16] for T2D subjects independently from the insulin delivery method. CGM recordings allows for direct observation of glycemic excursion and daily profile (unlike SBMG, and Hba1c measurements), that could inform about treatment effectiveness and possible lifestyle changes which must be done by the user[18]. Moreover, this signal allows to infer better quality information on glucose variability and on hypo- and hyperglycemia pattern[16]. However, potential drawbacks include the need to be actively used to be effective, and it could have accuracy limitation, especially with delay in recording BG changes in dynamic situation[18].
On the other hand, effective use of CGM metrics requires a correct interpretation of user data by medical doctors and this requires: common metrics assessment of CGM glycemic status, graphical visualization of the glucose data and CGM daily profile and clear clinical target.[16] Table 1.1 shows 10 metrics which may be most useful in clinical practice.

CGM metrics	
1. Number of days CGM worn (recommend 14 days)	
2. Percentage of time CGM is active (recommend 70% of data from 14 days) (41,42)	
3. Mean glucose	
4. Glucose management indicator (GMI)	
5. Glycemic variability (%CV) target #36%	
6. Time above range (TAR): % of readings and time .250 mg/dL (.13.9 mmol/L)	Level 2
7. Time above range (TAR): % of readings and time 181–250 mg/dL (10.1–13.9 mmol/L)	Level 1
8. Time in range (TIR): % of readings and time 70–180 mg/dL (3.9–10.0 mmol/L)	In range
9. Time below range (TBR): % of readings and time 54–69 mg/dL (3.0–3.8 mmol/L)	Level 1
10. Time below range (TBR): % of readings and time ,54 mg/dL (,3.0 mmol/L)	Level 2

Table .1.1 Standardized CGM metrics for clinical care: 2019[16]

Moreover, is also fundamental to adapt target percentages to special diabetes populations (e.g., pregnancy, high-risk) for providing a safer and more effective therapeutic decision making[16].
The metric defined included three CGM measurement:

- Time in range (TIR), percentage of readings and time within target glucose range.
- Time below range (TBR), time below target glucose range.
- Time above range (TAR), time above target glucose range.

Additionally, the consensus was reached on glycemic cut point for defining the TIR for T2D subject, 70-180 mg/dL or [3.9-10.0 mmol/L], along with the definition of cut points in the amount of time that T2D subject should eventually spend in each glycemic range. The percentage of time per day that should be strived by the patients are showed in table 1.2.
It would be important to prove that the time metrics of the CGM could predict clinical outcomes, so longer-term studies should be conducted in order to understand how the time spent in the different glycemic range correlates to diabetes complications. However different studies show the inverse correlation between TIR and the development of diabetes complications[19,20] as well its relationship with Hba1c[21,22].

	TIR		TBR		TAR	
Diabetes group	% of readings; time per day	Target range	% of readings; time per day	Below target level	% of readings; time per day	Above target level
Type 2	>70% >16 h, 48 min	70-180 mg/dl (3.9-10.0 mmol/L)	<4%; <1 h <1%; <15min	<70 mg/dL (3.9 mmol/L) <54 mg/dL (<3.0 mmol/L)	<25% <6h <5%; <1 h, 12min	>180 mg/dL (>10.0 mmol/L) 250 mg/dL (>13.9 mmol/L)
Older/high-risk type 2	>50% >12	70-180 mg/dL (3.9-10 mmol/L)	<1%; <15 min	<70 mg/dL (<3.9 mmol/L)	<10%; <2h, 24min	>250 mg/dl (13.9 mmol/L)

Table 1.2. Guidance on target assessment of glycemic control for adults with type 2 diabetes and older/high-risk individuals[16]

1.4 Aim

The purpose of this thesis is to make evident the already discussed limitations of the current basal-insulin titration. In fact, today one of the most used surrogate markers is the glycated hemoglobin (HbA1c) used for recognizing T2D subjects who can develop long-term diabetes complications. HbA1c reflects the average glucose over the last 2-3 months, furthermore it is an indirect measure of the average glycemia and, as such, it has some limitations. Moreover, the HbA1c is correlated to frequent SMBG[23], however this technique is invasive, unpleasant, and painful. Additionally, as previously mentioned this will not provide a continuous monitoring process, instead will require multiple daily testing in order to manage high glucose level[15].

As a result, the main goal of this work was to develop a new basal insulin titration rule based on more complete and extensive information, such the CGM signal, which as the SBMG is correlated to HbA1c levels[23]. From the CGM signal, to finetune the decision process, different time metrics are computed, such as a metric that indicates the time spent in range (TIR), one that indicates the amount of time above the target range (TAR) and metrics that describe the time spent below the target range (TBR); further details are provided in the section 1.3. Furthermore, by having more powerful information, the rationale is also to make a quicker titration process in those subjects that require, a higher insulin dose due to their characteristics.

1.5 Thesis Content

In the *Methods* section, it is briefly described the database and the T2D simulator and how the IDeg kinetics equations are integrated within the simulator. Following, a nod is done on the in-silico cloning of virtual populations. Then, a classifier is presented, which is used for discriminating between HIN and LIN. Subsequently, the state of the art of basal titration rule is outlined (i.e., DUAL I), then a detailed description of the common features of the new algorithms is reported and followed by the description of each version of the algorithm, characterized by one or more new features that improves their decision-making process. Finally, the best one is selected, and its *Results* are showed and commented in the *Discussion*, where the limitations of the method are also presented. The last part of the *Discussion* also includes the possible future improvements.

CHAPTER 2

METHODS

In this section of the thesis the method part is described. Firstly, it is presented a description of population used for carrying out the simulation. Then, the type 2 diabetes simulator (T2DS) is described. In particular, the system identification and the equations describing the glucose and insulin kinetics are outlined. Moreover, since the purpose of this work regards the basal insulin titration, the integration of the IDeg insulin equations is proposed to the reader.
Then, a nod is done to the in-silico cloning of the population, which is a fundamental part of the in-silico trial. Then, a machine learning approach used to classify subjects based on their insulin need, is presented. In fact, it makes sense to use more aggressive titration rule in those subjects who need higher doses (HIN) and be more cautious with those who need lower doses (LIN), but, this information is not known a priori, and for this reason a classifier which discriminates between HIN and LIN is needed.
Then, a brief description of the IDeg titration rules setup implemented in the T2DS is presented followed by the state-of-the-art titration-rule (DUAL I). Hence, the new algorithms are described, starting with the common parts containing filtering and feature extraction performed on the CGM signal and finally, each of the four versions of the algorithm is described in detail.

2.1 Database

The database used in this study consisted in an *in-silico* population (N=300), obtained using the method reported in [24] (described in detailed in section 2.3) to match the population described in[25]. Holst et.al.[25] study involved a cohort of 260 patients from the DUALI trial (122 female, Age = 55±9 years, BMI = 32.4±4.5 kg/m^2) which was used to tune the T2Ds to an insulin-naïve type 2 diabetes (T2D) population. Subjects was randomized in three treatment arms, IDegLira, IDeg or Liraglutide, and two standardized meal test was administered: before (visit 1) and at the end of a 26-week period in which once-daily treatment was given (visit 2); in each visit subject consumed a single, standardized, liquid meal containing ~96 g of carbohydrates. The concentration of plasma glucose, insulin and C-peptide were measured at different time instants. In Table 2.1, the population baseline characteristics are reported. Moreover, the simulated response of the above-mentioned population (N = 300) is represented below in Fig. 2.1.

Population Characteristics (N = 300)	**Mean ± SD**
BMI (kg/m^2)	31±4.6
Basal glucose (mg/dl)	167±24.84
Basal Insulin (pmol/L)	72±32.38
Basal C-peptide (pmol/L)	952±300.31
#Male	103
#Female	197

Table 2.1 Population baseline characteristics reported as mean±SD.

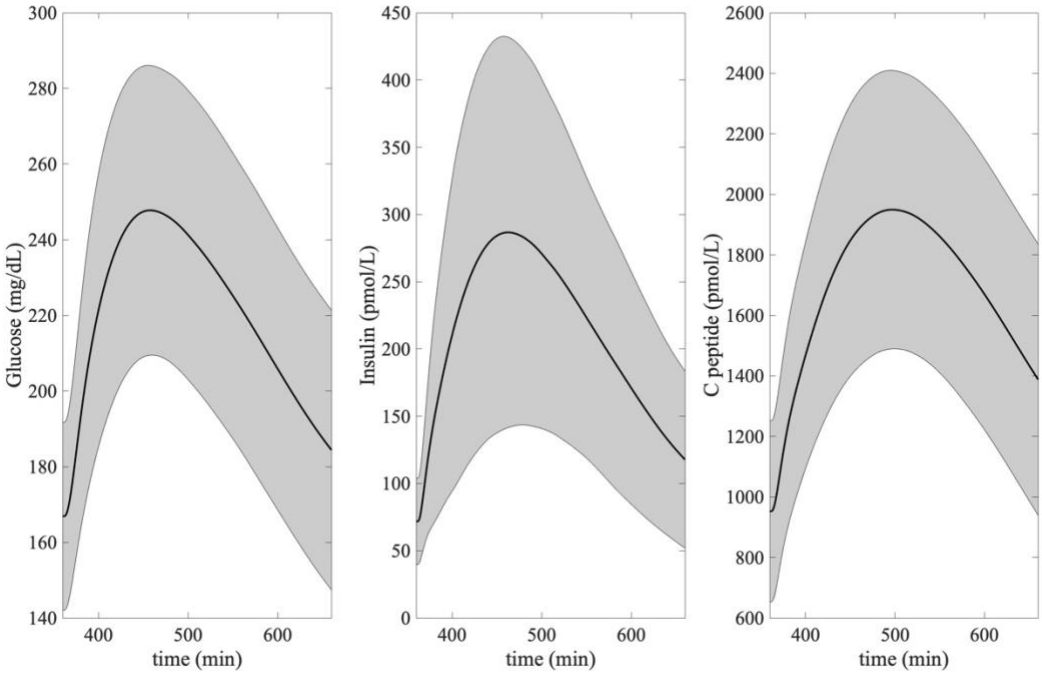

Figure 2.1. Simulated mean±SD (black line and gray areas) glucose (left), insulin (center) and c-peptide (right) concentrations of the population (N = 300) in response to the administration of a meal containing ~75 g of carbohydrates.

2.2 T2D Simulator

In silico trials, also known as virtual clinical trials, are customized and individualized computer simulations that are used to assess a medical product, device, or intervention offering significant advantages over current in vivo animal clinical trials.
Thus, in silico trials are a fundamental part of the 3 Rs approach (Replacement, Reduction, and Refinement) which go for a more respectful use of laboratory animals[27].
The T2Ds is a milestone in this field since it allows to simulate the glucose-insulin dynamics in T2D subject using a meal simulation model of glucose, insulin and C-peptide made of 15 differential equations and 39 parameter which was identified in Visentin et al.[28] using a system decomposition and forcing function Bayesian strategy on data of 51 T2D subject.
The model showed in the fig. 2.2 represent the transit of the glucose through the gastrointestinal tract, how the action of insulin influence the glucose utilization and its endogenous production, as well as the control applied by the glucose on the insulin secretion[28]. The model derives from that proposed by Dalla Man et al. [29]

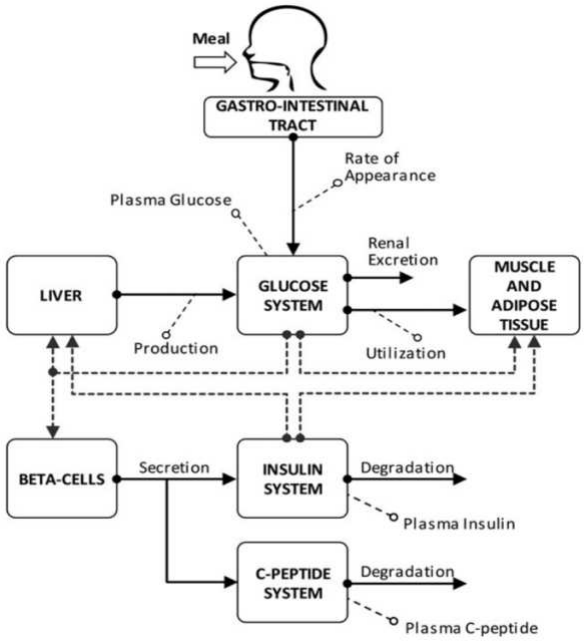

Figure 2.2 Figure from Visentin R., et.al. Diabetes Technol. (2020). Scheme of the T2D simulation model. Continuous lines indicate metabolic fluxes, while dashed lines represent control actions[28].

Like in the original model the glucose subsystem is described by a 2-compartment model: the first one indicates the glucose mass in plasma and rapidly equilibrating tissues G_p (mg/kg), the second compartment indicates the glucose mass in the slowly equilibrating tissues G_t (mg/kg), lastly the glucose plasma G (mg/dl) is considered as the output of this model (fig. 6). The model Equation are shown in (2.1) below.
The suffix b denotes a basal state; the EGP is the glucose endogenous production (mg/kg/min); Ra is the glucose rate of appearance in plasma (mg/kg/min); E is the renal excretion (mg/kg/min); U_{ii}

and U_{id} are the insulin-independent and -dependent glucose utilizations respectively (mg/kg/min); V_G is the distribution volume of the glucose (dl/kg); k_1 and k_2 (min^{-1}) are the rate parameters.

$$\begin{cases} \dot{G}_p(t) = EGP(t) + Ra(t) - U_{ii} - E(t) - k_1 \cdot G_p(t) + k_2 \cdot G_t(t) & G_p(0) = G_{pb} \\ \dot{G}_t(t) = -U_{id}(t) + k_1 \cdot G_p(t) - k_2 \cdot G_t(t) & G_t(0) = G_{tb} \\ G(t) = \dfrac{G_p}{V_G} & G(0) = G_b \end{cases} \quad (2.1)$$

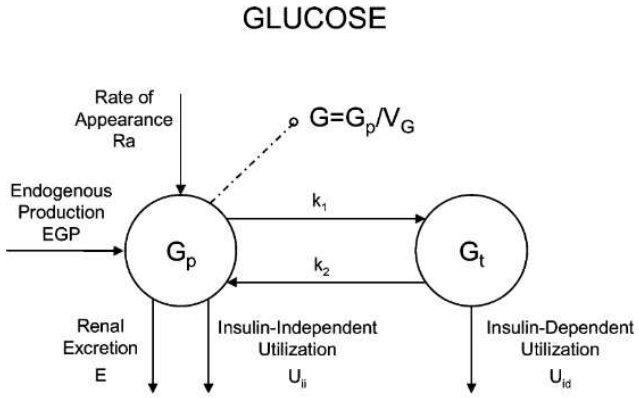

Figure 2.3. compartmental model used by Dalla Man et al.[29] for describing the glucose PK.

Furthermore, Dalla Man et. al[29] described the insulin kinetics using a two-compartmental model which is shown in fig. 2.4, where I_p (pmol/kg) is the insulin mass in the plasma and I_l (pmol/kg) is the insulin mass in the liver; I (pmol/L) is the plasma insulin concentration, and the suffix b stands for basal; S is the insulin secretion (pmol/kg/min); V_I is the distribution volume of the insulin (l/kg), and m_1, m_2 and m_4 are rate parameters (min^{-1}). The equations are showed in (2.2) below.

$$\begin{cases} \dot{I}_L(t) = -\big(m_1 + m_3(t)\big) \cdot I_L(t) + m_2 I_p(t) + \dfrac{S(t)}{BW} & I_L(0) = I_{Lb} \\ \dot{I}_p(t) = -(m_2 + m_4) \cdot I_p(t) + m_1 I_L(t) & I_P(0) = I_{pb} \\ I(t) = \dfrac{I_p(t)}{V_L} \end{cases} \quad (2.2)$$

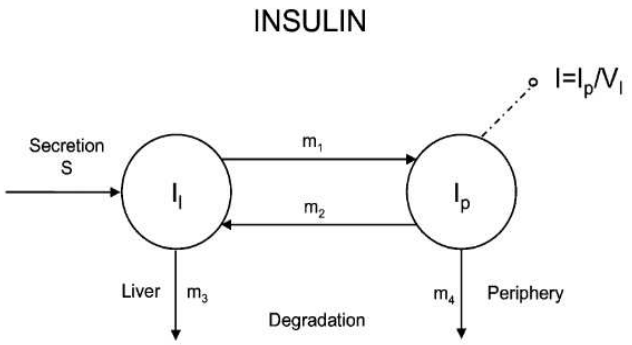

Figure 2.4. compartmental model used by Dalla Man et al.[29] for describing the insulin kinetic.

Where BW is the individual bodyweight (kg). In this model m_1, m_4 are the rate parameters to be estimated, m_2 is fixed to 0.268 min^{-1} and m_3 (min^{-1}) is a time-varying parameter which, according to Dalla Man et al.[29]:

$$m_3(t) = \frac{HE(t) \cdot m_1}{1 - HE(t)} \qquad (2.3)$$

HE is the hepatic insulin excretion, In the basal state:

$$I_{pb} = I_b \qquad (2.4)$$

$$I_{Lb} = \frac{m_2 \cdot I_{pb} + S_b/(BW)}{m_1 + m_3(0)} \qquad (2.5)$$

Where:

$$m_3(0) = \frac{HE_b \cdot m_1}{1 - HE_b} \qquad (2.6)$$

Moreover, is possible to obtain the basal and the total index of the hepatic insulin excretion:

$$HE_b = \frac{\frac{S_b}{BW} - m_4 \cdot I_{pb}}{\frac{S_b}{BW} + m_2 \cdot I_{pb}} \qquad (2.7)$$

$$HE_{tot} = \frac{\int_0^T m_3(t)\, dt}{\int_0^T (m_3(t) + m_1)\, dt} \qquad (2.8)$$

In the model also the hepatic sensitivity so insulin is considered:

$$S_I^{HE} = -\frac{\partial HE(t)}{\partial I}\bigg|_{ss} = a_I \qquad (2.9)$$

Where, the subscript ss indicates the steady state.

However, for describing the PK of the insulin in [28] they used a three- compartment model to represent the PK in the liver, in the plasma and in the extravascular space[30]:

$$\begin{cases} \dot{I}_L(t) = -\big(m_1 + m_3(t)\big) \cdot I_L(t) + m_2 I_P(t) + \dfrac{S(t)}{BW \cdot V_P} & I_L(0) = I_{Lb} \\ \dot{I}_P(t) = -(m_2 + m_4 + m_5) \cdot I_P(t) + m_1 I_L(t) + m_6 I_{EV}(t) & I_P(0) = I_{Pb} \\ \dot{I}_{EV}(t) = m_5 I_P(t) - m_6 I_{EV}(t) & I_{EV}(0) = I_{EVb} \\ I(t) = I_P(t) \end{cases} \quad (2.10)$$

In the *(2.11),* in which the only quantities that are not already defined for the *(2.2)* are m_5, m_6 which are rates parameters (min^{-1}), and I_{EV} is the insulin mass in the extra-vascular space.

Moreover, a model composed by two compartment is used for describing the kinetic of the C-peptide[31]:

$$\begin{cases} CP_1(t) = -(k_{01} + k_{21}) \cdot CP_1(t) + k_{12} \cdot CP_2(t) + \dfrac{ISR(t)}{V_C} & CP_1(0) = CP_b \\ CP_2(t) = k_{21} \cdot CP_1(t) - k_{12} CP_2(t) & CP_2(0) = CP_b \cdot k_{21}/k_{12} \end{cases} \quad (2.11)$$

Where CP_1 and CP_2 (pmol/L) are C-peptide concentrations in the accessible and in the peripheral compartment, CP_b (pmol/L) is the basal plasma C-peptide concentration, ISR (pmol/min) is the β-cell insulin (and C-peptide) secretion rate (like S(t) in *(2.11))*. V_C (L) is the C-peptide distribution volume in compartment 1 and k_{01}, k_{21}, k_{12} (min^{-1}) are transfer rate parameters.

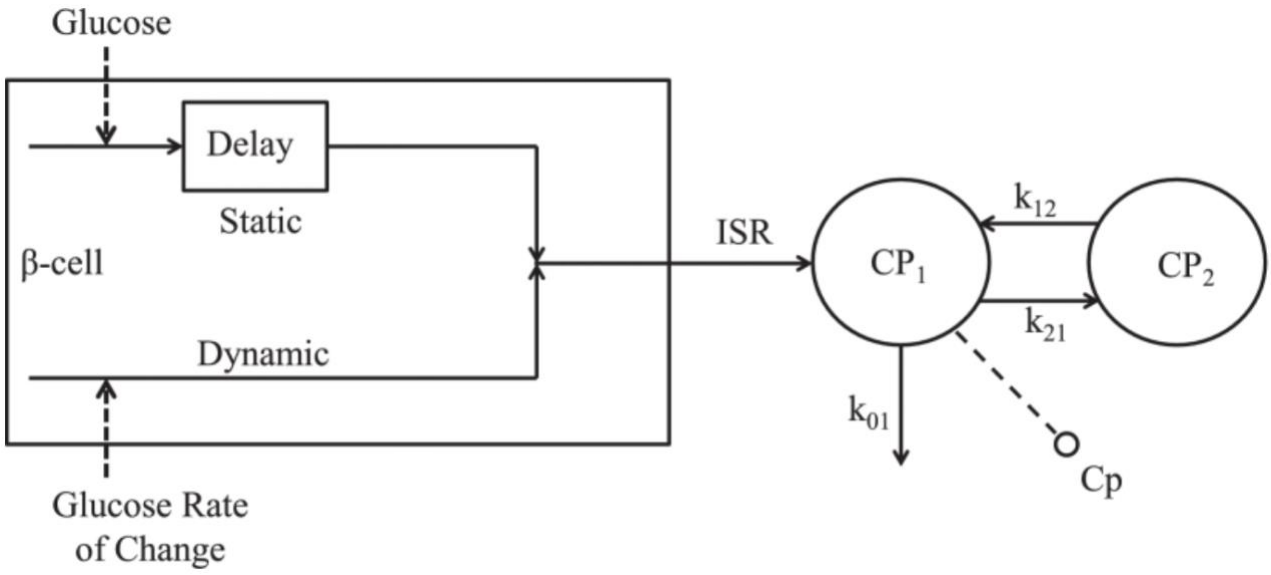

Figure 2.5. C-peptide secretion and kinetics model[30].

The following step is to integrate the equation that describes the PK of the subcutaneous absorption of IDeg into the T2DS, which is described by a three-compartment model [32]:

$$\begin{cases} \dot{I}_{q1}(t) = -k_d \cdot I_{q1}(t) + F \cdot D & I_{q1}(0) = 0 \\ \dot{I}_{q2}(t) = -k_d \cdot I_{q2}(t) + k_d \cdot I_{q1}(t) & I_{q2}(0) = 0 \\ \dot{I}_{q3}(t) = -k_a \cdot I_{q3}(t) + k_d \cdot I_{q2}(t) & I_{q3}(0) = 0 \\ Ra_I = k_a \cdot I_{q3}(t) \end{cases} \quad (2.12)$$

Where D (mU/kg/min) is the insulin dose administered subcutaneously, F (dimensionless) represent the bioavailability, k_d (min^{-1}) is the rate constant of molecular complex conversion, k_a (min^{-1}) is the rate constant of insulin absorption to plasma, and Ra_I is the insulin rate of appearance in plasma.
Then the PK of the IDeg was incorporated into the T2Ds model and the individual insulin PK parameters were obtained as a random realization of a joint parameter distribution created from T1D data and adapted to T2D by updating the average parameter vector[24].

2.3 In silico Cloning

The simulations used to test all the different versions of the algorithm are based on a virtual population in which each virtual subject is represented by a vector containing the model parameters, $\mathbf{p}$[28]:

$$\boldsymbol{p} = \left[p_1, p_2, \dots, p_{N_p}\right]^T \qquad (2.15)$$

where N_p indicates the number of the model parameter. There are different ways for defining this vector, one is to consider it as a realization of an appropriate joint parameter distribution, which under the assumption of normality, must be well represented by the average vector $\boldsymbol{\mu_p}$ and the covariance matrix $\boldsymbol{\Sigma_p}$. They were obtained by identifying the large-scale T2Ds model on data coming from both T2D and healthy subject. However, to make the T2Ds representative of an insulin-naïve T2D population an update of the joint parameter distribution is required. The flowchart explaining the tuning procedure is showed in Fig. 2.5).

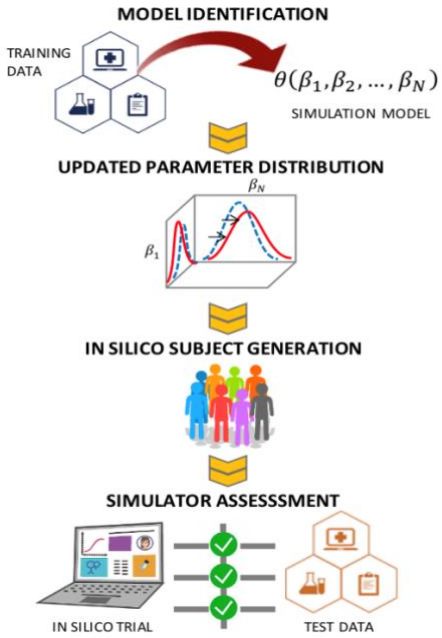

Figure 2.5. Flowchart of the tuning procedure to clone a desired T2DS population[24]

The up mentioned update was done in [24] by fitting the T2Ds model [28,29,33] with the average data coming from the first visit, hence before the treatment, available from [25]. The visit 1 was chosen to fit the models in order to identify, using the Maximum a Posteriori (MAP) estimator based on the prior of [28], population's key parameters, which describe the rate of absorption, insulin sensitivity and insulin secretion indexes[24]. These were used to update the parameter distribution means and then to generate the cohort of 300 subjects described in section 2.1.

2.4 Insulin Needs Classifier

One of the goals of the new algorithms is to reach the optimal basal insulin dose in a less amount of time for reducing the risk of long-term hyperglycemia related complication. However, to be able to achieve faster administration of optimal doses higher increments are needed, and it makes sense to apply more aggressive titrations only in those patients requiring them, thus those having a higher insulin demand. The reason behind the different insulin need can be due both to inter-subject variability in parameter characterizing the insulin response or because the subject has a complete deficiency in endogenous insulin production. However, this information is not a-priori known, therefore for distinguishing between a higher- or lower- demand subject a machine learning approach is used. In particular, the classifier proposed by Bonet et al.[26] was used. The data were generated by the T2Ds simulator using the same population of this thesis. The in-silico subject underwent two experiments, the first was a standard oral glucose tolerance test (OGTT), while the second was a standard 52-week basal insulin titration trial (DUAL I) to find the subject-specific optimal degludec insulin dose (OID), starting from 10 U. The up-titrating process was FPG based and the dose adjusting was done twice a week (+2U or -2/-4U) depending on the distance on the measured FPG from the range [70-90] mg/dl.
Once the OID was found for each subject, they were divided in 2 insulin needs classes: high insulin need (HIN) if OID≥ 44 U, and low insulin need (LIN) otherwise. They developed a logistic regression model to apply the mentioned classification using some measurable features, the model equation is:

$$logit(P) = ln\left(\frac{P}{1-P}\right) = \beta_0 + \sum_{j=1}^{N} \beta_j X_j \qquad (2.16)$$

Where P is the probability to classify subjects as HIN, $\beta = [\beta_0, \beta_1, \dots, \beta_N]$ is the vector of the model coefficient, β_0 is the intercept while β_j is the parameter assigned to the X_j feature. For this purpose, as input features were considered sex, BW, BMI, age and the baseline plasma glucose, insulin and C-peptide concentrations, measured at 0 minutes (subscript 0), 120 minutes (subscript 120) and 180 minutes (subscript 180) after glucose intake.
In the first place a 70/30 split between the training set and test set of the original dataset was performed. Then, a feature selection was done using a 100-bootstrap-resampling of the training-set. During the training, the models were kept, in which all features were statically significant in at least 70 % of the internal training sets and at the same time the average deviance was statically different from the one of the null model (i.e., model in which only the intercept is considered).

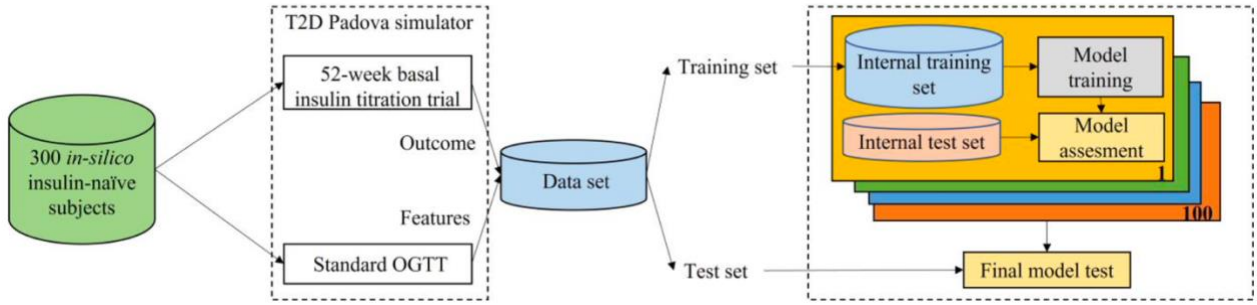

Figure 2.6 schematic representation of models training and testing procedures[26]

During the training phase, a grid-search approach was used in each internal test set for defining the optimal P_{th} , which is then used in *(2.25)* as the cut off probability for the classification rule:

$$P_{th} = argmax_P(mean(Sensitivity) \cdot mean(Specificity)) \qquad (2.17)$$

With the $Sensitivity$ and the $Specificity$ defined as follows:

$$Sensitivity = \frac{TP}{TP + FN} \qquad (2.18)$$

$$Specificity = \frac{TN}{TN + FP} \qquad (2.19)$$

With TP the number of true positive, FN the number of false negative, TN the number of true negative and FP the number of false positive. The $Sensitivity$, the $Specificity$ and the AUC-ROC was used also in the model testing, furthermore the other performance metrics was calculated such as:

$$Precision = \frac{TP}{TP + FP} \qquad (2.20)$$

$$Accuracy = \frac{TP + TN}{TP + FP + TN + FN} \qquad (2.21)$$

$$F1 - score = \frac{2TP}{2TP + FP + FN} \qquad (2.22)$$

Moreover, the area under the receiver operating characteristic curve (AUC-ROC) was computed using the internal test sets, and the model with the highest average AUC-ROC was selected.
Among the candidate logistic models, the one chosen has as covariates the subject OGTT glucose and C-peptides measurements:

$$logit(P) = -5.2351 + 0.0742 \cdot G_0 - 0.0389 \cdot G_{180} + 0.003 \cdot Cp_0 - 0.0038 \cdot Cp_{120} + 0.0036 \cdot Cp_{180} \qquad (2.23)$$

After the training phase the developed model *(2.23)* was used in the test set. For each subjects the estimated probability was:

$$\hat{P} = \frac{exp(logit(P))}{1 + exp(logit(P))} \qquad (2.24)$$

And the classification rule was:

$$\begin{cases} HIN & if\ \hat{P} > P_{th} \\ LIN & if\ \hat{P} \leq P_{th} \end{cases} \qquad (2.25)$$

Where P_{th} is the threshold probability, determined in the in the model training phase *(2.17)*. The performances of the model are shown in the table 2.2.

Performance metrics	**Model performance**
Sensitivity	87%
Specificity	91%
Precision	91%
Accuracy	89%
F1-score	0.89
AUC-ROC	0.94

Table 2.2 Model performances of the model (22)

2.5 IDeg titration Rules

In order to assess the efficacy of different titration rules we used the DUAL I[11] as . A 1-year in silico trial has been performed, in which each insulin-naïve HIN T2D subject assumed 3-meal/day. The starting dose was setted at 10 U, as recommended by ADA[12], and adjusted every 3 days. Insulin dose was gradually increased until reaching an individualized optimal dose but the update process, the parameters evaluated for deciding whether to administer an increment/decrement and their magnitude depend on the specific rule.

2.5.1 DUAL I

As common practice, literature therapy is simulated and considered as the baseline to compare with the new algorithm. As previously discussed in the section *2.4*, during the in-silico trial the dose was changed every 3-day following the indication provided by the DUAL I rule, which is implemented in the T2Ds.
Firs, the titration algorithm assumes a prebreakfast glucose (FPG) target between ~72 mg/dL and ~90 mg/dL, furthermore 3 hypoglycemic thresholds were defined: the first one at 70 mg/dL, the second at 60 mg/dL and the last one at 50 mg/dL, the last one marking a severe hypoglycemic event; moreover, each BG threshold is coupled with a maximum percentage of time which can be spent by the subject below it. For the first the threshold is 7.5%, for the second 5% and for the third threshold is 2.5%, these values correspond to ≈8% tolerance which is almost 2 hours per day.
The rule bases its dose adjustment just on the value of the FPG, in fact:

- If FPG is lower than 72 mg/dL, which is the lower bound of glucose target range, the subject is considered in hypoglycemia, hence the dose is decreased by 2 U or by 4 U based on the

gravity of the hypoglycemic event: if the first two thresholds are overcome, the new dose proposed to the subject is decreased by 2 U, while if the tolerance time threshold associated to 50 mg/dL is overcome the decrement administered is 4U.

- If FPG is greater than 90 mg/dL, which is the upper bound of glucose target range, the subject is considered in hyperglycemia, hence the dose is increased by 2 U.
- Within the rule, it is also implemented a system to evaluate if a possible severe hypoglycemic event has occurred.

Average FPG values are then computed over a period of 3 days, and this process is repeated until the rule finds an optimal insulin dose, i.e. a dose that keeps the prebreakfast glucose of the subject in the range [72-90] mg/dL without causing hypoglycemia. This optimal dose is personalized in the sense that each subject requires a specific amount of insulin to reach the prebreakfast glucose target. Indeed, this is influenced by the inter- and intra- subject variability and also by different parameters which modify the insulin response of the subject, such being pathologically overweight[34], this typically induces insulin resistance[34] hence lowering the insulin sensitivity of the subject leading to higher treatment difficulties.

2.5.2 New Titration Algorithms

In this section the new 4 tested rules are presented. The features common to all the algorithms are outlined first. Then, each of them is described in detail. Figures 2.9 ,2.12, 2.16 and 2.19 show a schematic representation of algorithms 1, 2, 3, and 4 respectively.

2.5.2.1 Common features

As previously discussed, DUAL I dose adjustment is based on evaluation of FPG. Moreover, it does not take into account how the glucose concentration varies during the day, the decision boundaries which are applied to the subject FPG values are not individualized and based on the ADA guidelines[12].

The new algorithms were implemented to not consider just a single, or a small set, of values coming from the SMBG, the goal was to make a more extensive and accurate evaluation on how the patient glycemia changes during the day. Each new algorithm uses as input the 3-days simulated CGM, (see *Introduction* section 1.3), and as output the new proposed insulin dose which satisfies certain criteria. Each titration algorithm is based on the evaluation of the CGM signal, provided by the T2Ds, which is processed to extract some characteristics to better understand the glycemic status through the 3-days period.

The simulated CGM has some noise superimposed on it, which could compromise the following steps, for this reason a filtering step was applied first. The filtering operation chosen is the gaussian smoothing. Firstly, for doing a smoothing operation, and then for each point, the value of the kernel function (i.e., a function that taking 2 vector returns a scalar, which typically is the dot-product of the 2 input vectors taken to a higher dimension space) is calculated, hence the weighted average of data point is computed by using as weights the kernel function values. In practice, the data points of the CGM signal are modified so that the individual points that are higher than the adjacent points are reduced, and points that are lower than the adjacent points are increased. In gaussian smoothing the kernel used is Gaussian:

$$K(x^*, x_i) = \exp\left(-\frac{(x^* - x_i)^2}{2b^2}\right) \qquad (2.26)$$

where b defines the width of the kernel, x_i are the data point and x^* is their mean, thus the $(x^* - x_i)^2$ term is the squared Euclidean distance. The reason behind choosing such a filtering operator is because it is able to achieve a tradeoff between successfully removing the high frequency noise superimposed on the CGM signal and not filtering lower-frequency information which are related to the subject glycemia variation due to a meal or to a physical activity.

After filtering the signal, another signal processing operation is performed on the CGM. Specifically a trend decomposition process using the singular spectrum analysis (SSA)[35]. The SSA is a nonparametric technique that works with arbitrary statistical processes, whether linear or nonlinear, stationary or non-stationary, Gaussian or non-Gaussian[36]. Hence, it is a very general technique which studies the "separability" that characterizes how well different signal components can be separated one from each other.

Furthermore, real time series, such as the CGM, usually have a complex structure and time varying dynamics. Thanks to its properties, the SSA method works best when applied to real world signals such as the up mentioned CGM[36].

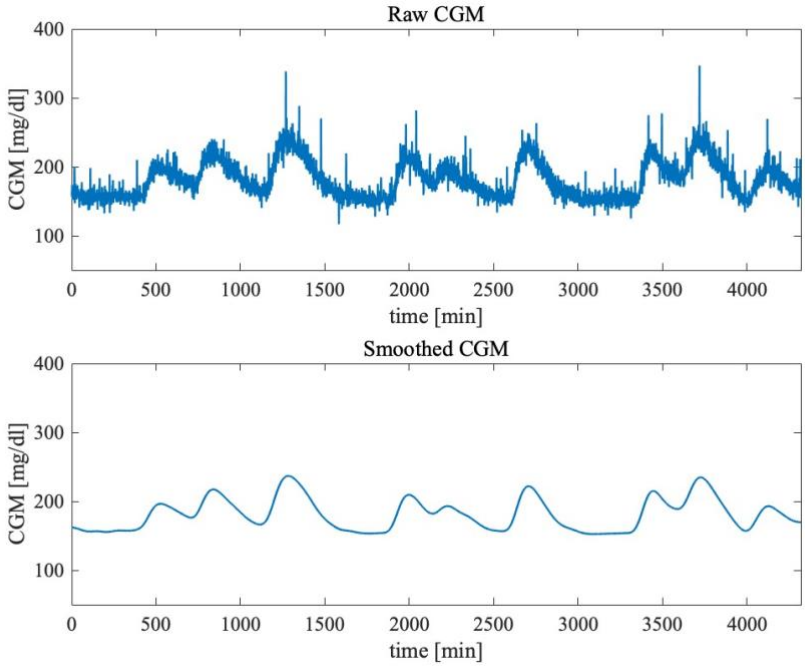

Figure 2.7 Smoothed (upper panel) and original (lower panel) CGM signal after filtering using a Gaussian kernel

Here it follows a briefs description of the SSA algorithm:

Let consider a time series $Y_T = (y_1, \dots, y_r)$. Fix L $(L \leq T/2)$, the window length, and let $K = T - L + 1$:

Step 1. *(Computing the trajectory matrix)*: this transfers a one-dimensional time series $Y_T = (y_1, \dots, y_r)$ into a multi-dimensional series $X_1, \dots, X_k$ with vectors $X_i = (y_i, \dots, y_{i+L-1}) \in \mathbb{R}^L$, where

$K = T - L + 1$. The single parameter of the embedding is the window length L, an integer such that $2 \leq L \leq T$. The result of this step is the trajectory matrix $\boldsymbol{X} = [X_1, \dots, X_k]$:

$$\boldsymbol{X} = (x_{ij})_{i,j=1}^{L,K} = \begin{pmatrix} y_1 & y_2 & y_3 & \cdots & y_K \\ y_2 & y_3 & y_4 & & y_{K+1} \\ \vdots & & & \ddots & \vdots \\ y_L & y_{L+1} & y_{L+2} & \cdots & y_T \end{pmatrix} \qquad (2.27)$$

Note that the trajectory matrix $\boldsymbol{X}$ is a Henkel matrix, which means that all the elements along the diagonal $i + j = constant$ are equal.

Step 2. *(Constructing a matrix for applying the singular value decomposition [SVD])*: compute the matrix $\boldsymbol{XX^T}$**.**

Step 3. *(SVD of the matrix $\boldsymbol{XX^T}$)*: compute the eigenvectors of the matrix $\boldsymbol{XX^T}$, and consider $\boldsymbol{XX^T} = P\Lambda P^T$. Here $\Lambda = \text{diag}(\lambda_1, \dots, \lambda_L)$ is the diagonal matrix of eigenvalues of $\boldsymbol{XX^T}$ ordered as $\lambda_1 \geq \lambda_2 \geq \cdots \geq \lambda_L \geq 0$ and $P = (P_1, P_2, \dots, P_L)$ is the corresponding orthogonal matrix of eigen-vectors of $\boldsymbol{XX^T}$.

Step 4. *(Selection of eigen-vectors)*: select a group of l $(1 \leq l \leq L)$ eigen-vectors $P_{i1}, P_{i2}, \dots, P_{il}$.
The grouping step correspond to splitting the elementary matrices $\boldsymbol{X}$, into several groups and summing the matrices within each group. Let $I = \{i_1, \dots, i_l\}$ be a group of indices $i_1, \dots, i_l$. Then the matrix $\boldsymbol{X}_I$ corresponding to the group I is defined as:

$$\boldsymbol{X}_I = \boldsymbol{X}_{i_1} + \cdots + \boldsymbol{X}_{i_l} \qquad (2.28)$$

Step 5. *(Reconstruction of the one-dimensional series)*: compute the matrix:

$$\widetilde{\boldsymbol{X}} = \left\| \tilde{x}_{i,j} \right\| = \sum_{k=1}^{l} P_{ik} P_{ik}^T \boldsymbol{X} \qquad (2.29)$$

As an approximation to $\boldsymbol{X}$. Transition to the one-dimensional series can now be achieved by averaging over the diagonals of the matrix $\widetilde{\boldsymbol{X}}$.

In MATLAB these steps are implemented by using *trenddecomp.m* function which finds trends in a vector of data (i.e., CGM) by considering them as an additive decomposition:

$$CGM = LT + ST + R \qquad (2.30)$$

Where:

- LT is the long-term trend in the data.
- ST is the seasonal, or oscillatory, trend (or trends).

- R is the remainder (i.e., what is left of time series data after removing the long-term component and the seasonal components, thus is the random fluctuation that cannot be explained by the other trends).

For the sake of this work just the long-term (LT) trend is considered. In fact, the rationale was to understand whether the trend of the CGM was rising or not during the simulated 3 days. Thus, a possible way for getting this information was to evaluate the mean slope of the LT trend. Defining the first order interpolating polynomial as:

$$y_{int} = p_1 \cdot t + p_2 \qquad (2.31)$$

y_{int} is the value of the polynomial function, p_1 is the mean slope of the polynomial, hence the LT trend average slope and p_2 is the intercept on the y-axis. A graphical representation is shown in figure 2.8. However, since the computation of the mean slope is affected by an error, this must be considered to understand whether the trend is significantly positive, negative or indistinguishable from zero.

First, the residuals are computed as:

$$r = CGM_{smoothed} - y_{int} \qquad (2.32)$$

Then the degrees of freedom:

$$df = N_{CGM} - 2 \qquad (2.33)$$

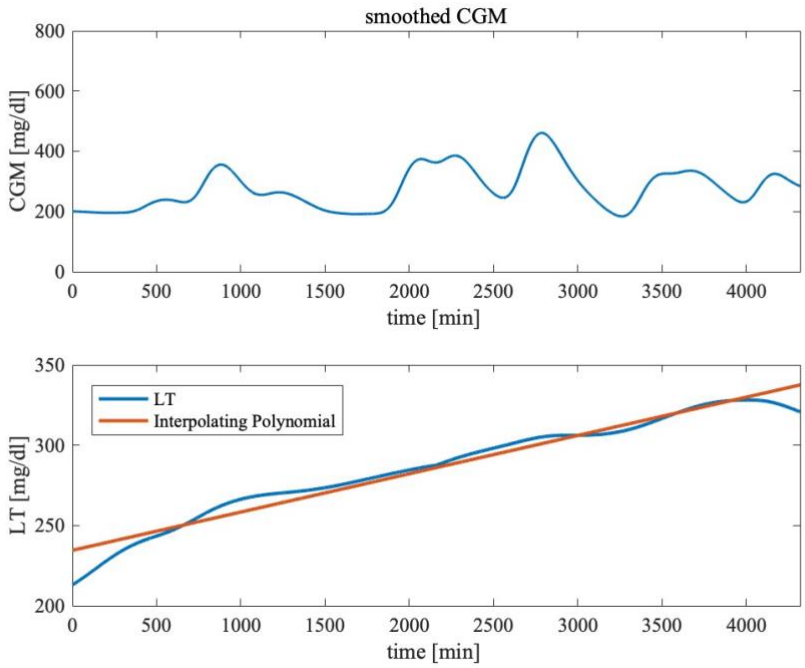

Figure 2.8 Smoothed CGM (upper panel), and CGM LT trend (lower panel) with the first-grade interpolating polynomial

where N_{CGM} is the number of samples of the CGM. Then, the standard error of the slope estimate is computed:

$$s = \sqrt{\sum_i \frac{r(i)^2}{df}} \qquad (2.34)$$

Then, considering the *(2.34)*:

$$Se = \frac{s}{\sqrt{\sum_i \left(t(i) - avg(t)\right)^2}} \qquad (2.35)$$

Knowing the slope estimate standard error, one can retrieve the correspondent t-value:

$$t = \frac{p_1}{Se} \qquad (2.36)$$

From the value of the functional t the correspondent p-value can be extracted from the t-student cumulative probability density function[37]; this will be used to understand whether the slope is significantly positive or negative, therefore this information is used for understanding if the glycemia of the subject is significantly rising or not, hence algorithms can recognize if the subject needs an incremented new insulin dose.
One of the main difference that characterizes these new algorithms is the calculation and the evaluation of 4 different time metrics which are computed from the raw CGM and are almost the same defined by the ADA [18]:

1) Time in range (TIR), which is the time that the subject spends, during the 3 days, between 70 mg/dl and 180 mg/dl (3.9 mmol/L-10.0 mmol/L).
2) Time in hypo 1 (TH1), which is the time that the subject spends, during the 3 days, between 60 mg/dl and 70 mg/dl (3.4 mmol/L-3.9 mmol/L).
3) Time in hypo2 (TH2), which is the time that the subject spends, during the 3 days, between 50 mg/dl and 60 mg/dl (2,8 mmol/L-3.4 mmol/L).
4) Time in severe hypo (TSH), which is the time that the subject spends, during the 3 days, below 50 mg/dl (0 mmol/L-2.8 mmol/L).

It is easy to understand that considering this metrics instead of the FPG provides a more complete and powerful information for better understanding and managing eu/hyper/hypo glycemia. Moreover, they are coherent to Battelino et al.[16], (*Introduction*, section 1.3), on the importance of having a metric which indicates a glycemic target (TIR), metrics that characterize the time spent by the subject below the target (TH1, TH2, TSH), and also metrics which define the time above the glycemic target (TAR). Despite there is not an explicitly defined TAR, it can be easily retrieved knowing both the TIR and TBR information.
As seen in DUAL I, time thresholds are applied to the hypoglycemic time metrics (i.e., TH1, TH2, TSH), in particular the thresholds chosen are the same used in the DUAL I rule: TH1 should not exceed 7.5%, TH2 should not exceed 5 % and TSH should not be over 2.5%; thus, these values correspond to a tolerance of the 8 % which correspond to almost 2 hours per day.

Moreover, given that each version of the new algorithm uses all CGM samples collected during the last 3 days (i.e. this allows to not miss any hypo- or hyperglycemia), 8 different hypoglycemic cases are considered:

1) TH1<7.5%, TH2<5%, TSH<2.5%, euglycemia or hyperglycemia.
2) TH1≥7.5%, TH2<5%, TSH<2.5%, mild hypoglycemia.
3) TH1<7.5%, TH2≥5%, TSH<2.5%, moderate hypoglycemia.
4) TH1≥7.5%, TH2≥5%, TSH<2.5%, moderate hypoglycemia.
5) TH1<7.5%, TH2<5%, TSH≥2.5%, severe hypoglycemia.
6) TH1<7.5%, TH2≥5%, TSH≥2.5%, severe hypoglycemia.
7) TH1≥7.5%, TH2<5%, TSH≥2.5%, severe hypoglycemia.
8) TH1<7.5%, TH2<5%, TSH≥2.5%, severe hypoglycemia.

In addition, in each "severe hypoglycemia" case, a flag (*SevereHypo*) is set to 1 and the current dose will not be assigned to the subject anymore.
For the sake of argument, each version of the algorithm will be divided in 2 cases regarding the *ExitFlag*, i.e., a flag which indicates whether the optimal dose is found (*ExitFlag* = 1) or not (*ExitFlag* = 0). When the optimal basal-insulin dose is not found, the eight previously mentioned cases will be treated. Furthermore, each time metrics computed on the CGM (TIR, TH1, TH2, TSH) is composed of 3 values, one for each day.

2.5.2.2 Titration Algorithm 1

At the beginning, a *flag* is set to zero *(ExitFlag = 0)*

When *ExitFlag = 0*, it means that the optimal Dose has not yet been found. Therefore, the algorithm is asked to search a better basal-insulin dose. To do that, first, then algorithm tests if the subject is in eu- or hyperglycemia. If this is the case, the subject did not exceed the hypoglycemic threshold defined above (i.e., TH1, TH2 and TSH). The TIR is calculated and the following conditions may occur:

- *The current measured TIR is the highest obtained so far*

If 10%<TIR<95%, the LT trend of the smoothed CGM is computed and interpolated by a first-order polynomial. From *Eq 2.31,* the p_1 is evaluated as the mean slope of the LT trend. As discussed in *2.5.2.1,* the value of the t functional is computed (tvalue) and the corresponding p-value is obtained. This last is used for understanding if the p_1 estimate is statistically significant.

- If p_1*>0, p-value<0.05*

  In this case the average slope is significantly greater than zero, meaning that, on average, the LT trend based on 3-days CGM is raising. As a result, the algorithm increments the dose by 10 U to achieve at least the minimum clinically significant improvement in TIR (i.e., 5%)[16]
- If p_1*>0, p-value>0.05;* p_1*<0, p-value<0.05;* p_1*<0, p-value>0.05*

  In all this cases, the algorithm keeps the current dose

Moreover, if the maximum of the TIR vector is greater than 95%, the *ExitFlag* is set to 1 and the current dose is considered the optimal since no further clinically relevant improvement in TIR is possible. On the other hand, if the maximum of TIR is lower than 10% a doubled (20 U) increment is administered to significantly reduce the TAR, since it means that the subject is in a severe hyperglycemic state.

- *The current TIR is not the greatest obtained so far*

This case is interpreted by the algorithm as the subject cannot improve his TIR any further. If the previous maximum TIR was between 10% and 95%, the LT trend of the smoothed CGM is computed and interpolated by a first-order polynomial. Again, the p_1 is evaluated as the mean slope of the LT trend; the t-value is computes and the corresponding p-value is obtained.

- If p_1*>0, p-value<0.05*

  The information provided by the interpolation of the CGM-LT indicates that the CGM on average is still significantly rising, even if the current TIR is not the greatest and the subject has not experienced hypoglycemia. Thus, the algorithm proposes a 10 U increment to the dose. In this case, since the subject stopped his improvement phase, before administering the dose, the algorithm checks if the new dose is associated to previous severe hypoglycemic events: when the TSH tolerance threshold is exceeded, the *SevereHypo* flag is activated, hence the dose is associated to a severe hypoglycemic state and will not be administered anymore; if the previous severe hypoglycemic check is positive, then the current dose is kept, if the check is negative the incremented dose is proposed as new dose for the next iteration.
- p_1*>0, p-value>0.05;* p_1*<0, p-value>0.05*

In these two cases the information coming from the mean slope of the LT trend is not statistically significant, and since the subject is in an eu/hyperglycemia state the current dose is kept.

- $p_1<0$, *p-value<0.05*

The slope of the interpolating polynomial is significantly negative; therefore, the subject is not improving anymore, and its 3-days glycemic state trend on average is descending. However, since the goal of the algorithm is to maximize the TIR, due to the up mentioned conditions, a search of the past maximum TIR is done with its correspondent dose. However, before assigning it to the subject, the algorithm checks the value of the previous maximum TIR: if is lower of 50%, the search continues, in fact in this case the dose was not high enough to treat the hyperglycemia, bringing the subject to spend a major part of the time above the glycemic target range. While, if the maximum TIR is greater than 50% the dose associated to the previous maximum TIR is administered to the patient as optimal and *ExitFlag* is set to 1. The 50 % threshold on the time in range was set in agreement with what reported by Battelino et. al [16] as guidance on target for assessment on glycemic control for older/high-risk adult with type 2 diabetes.

If the previous maximum of the TIR is lower than 10%, the subject is in a marked hyperglycemic state, thus a 20 U incremented administered applied to the current dose to reduce the time spent above the target range. As last case, if the previous maximum TIR is greater than 95%, since is the last improvement which can be done by the subject, the correspondent dose is considered to be optimal (*ExitFlag* = 1) and is administered to the patient.

During the optimal dose search phase, also hypoglycemic events are managed, since there are three different time metrics which make the algorithm capable of recognizing the severity of the hypoglycemia and act accordingly. As discussed in the *Common parts* section 7, different possible situations are considered by each version of the algorithm and the proposed dose decrement is proportional to the severity of the hypoglycemic event.

- *TH1≥7.5%, TH2<5%, TSH<2.5%*

This is the lightest hypoglycemic state that the subject can experience. If this case occurs in the first iteration of the algorithm, a 2U decrement is assigned, while, if it occurs from the second iteration, the algorithm searches for the previous maximum TIR. However, before assigning the dose associated to the previous time in range the algorithm checks if the maximum TIR is associated to a TH1>7.5% and/or to a TH2>5%. If so, a 2 U decrement is administered to the subject, while, if the hypoglycemic tolerance thresholds are not exceeded the correspondent maximum TIR dose is proposed as new dose.

- *TH1<7.5%, TH2≥5%, TSH<2.5%*

Since the second time threshold is exceeded (i.e., associated to the [50-60] mg/dL range), the hypoglycemic event is considered more severe. Hence, the dose is decremented of 4 U

- *TH1≥7.5%, TH2≥5%, TSH<2.5%*

This is the other thresholds combination identifying a moderate hypoglycemic event. However, in this case, both the tolerance thresholds associated to the [60-70] mg/dL range and [50-60] mg/dl range are exceeded. Hence, since this is associated to a more severe hypoglycemia than the previous case, a 6 U decrement is administered to the subject.

- *TH1<7.5%, TH2<5%, TSH≥2.5%; TH1<7.5%, TH2≥5%, TSH≥2.5%; TH1≥7.5%, TH2<5%, TSH≥2.5%; TH1<7.5%, TH2<5%, TSH≥2.5%*

  These 4 different tolerance threshold combinations have in common the exceeding of the severe hypoglycemic threshold, associated to <50 mg/dL range. This kind of hypoglycemic events are very dangerous because they result in feeling shaky and confused, seizures, and death[38]. For these reasons, it is fundamental to minimize this kind of events. However, when they occur, the algorithm is strictly conservative thus it administers a 10 U decremented dose to raise the glycemia of the subject.

- *ExitFlag* = 1

The *ExitFlag* is set to 1 by the algorithm when a certain dose is considered to be optimal, and this is kept until at least one of hypoglycemic tolerance threshold is exceeded (i.e., TH1 ≥7.5% ∨ TH2≥5% ∨ TSH≥2.5%). In this case, the *ExitFlag* is set again to zero and the research, described in the previous part, restarts.

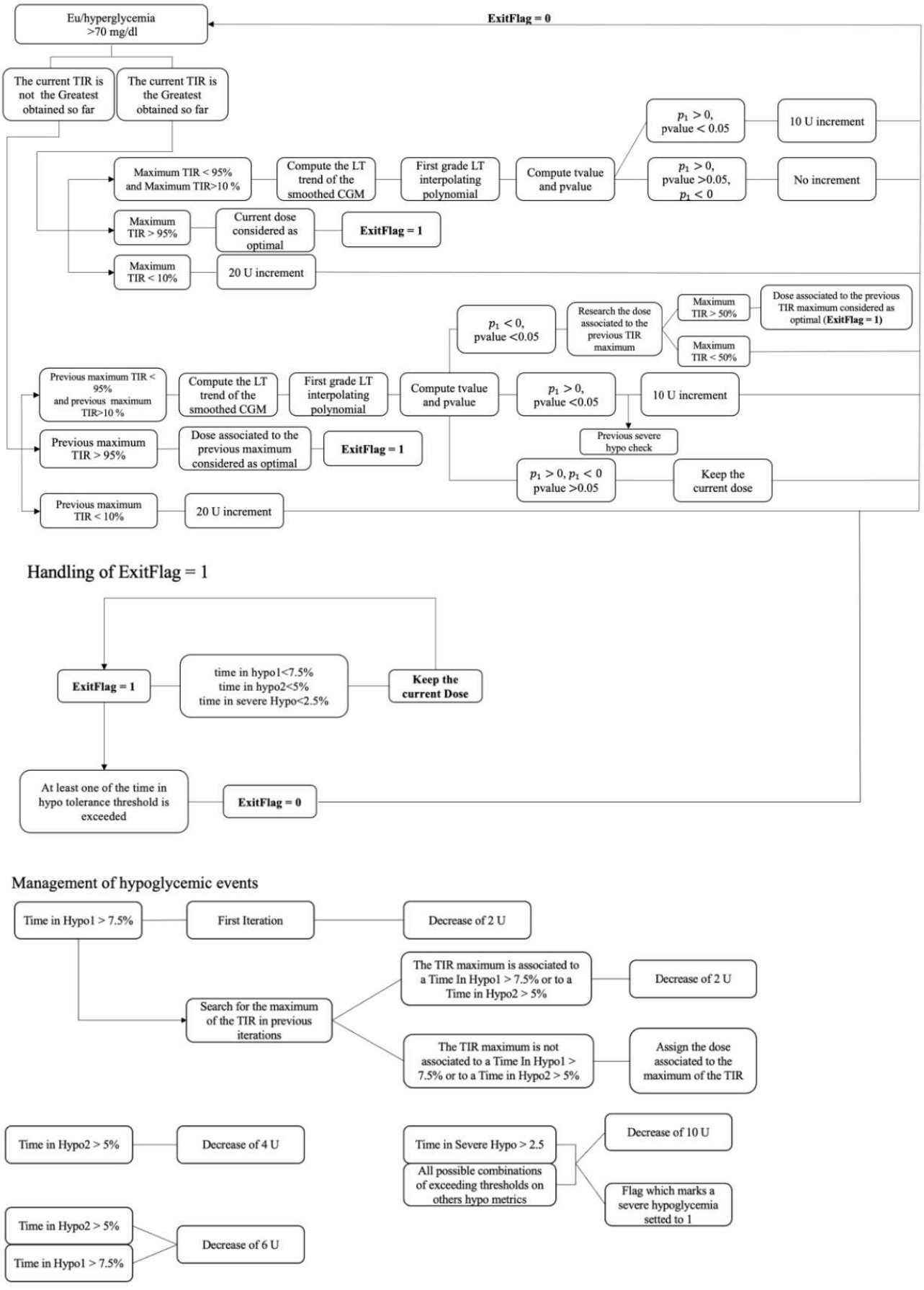

Figure 2,9 Flowchart of Algorithm 1, Eu/hyperglycemia management (above), handling of ExitFlag = 1 (middle) and management of hypoglycemic events (below)

2.5.2.3 Titration Algorithm 2

One of the main problems of the first version of the algorithm was its instability. In fact, due to subject glycemic variation, due to meal variability and/or to physical activity, the first version of the algorithm was proposing increment that led to recurrent hypoglycemic events. Hence, periodic increments were proposed to the subject bringing a higher insulin concentration that raises all the TBR metrics. In figure 2.10, an example of this behavior is shown.
Thus, one of the possible solutions was to implement a flag (*Back*) which marks when a previous administered dose is proposed again to the subject, a counter is then associated to each dose which is incremented when *Back* is setted to one, hence it represents how many times the dose is administered to the subject. When a dose is proposed for the third time throughout the entire trial, it is considered as optimal dose. Furthermore, *Back* is set to 1 when the severe hypoglycemia check prevents the 10 U increment, thus forcing the dose to remain at a certain value through different iterations without labeling it optimal, even if it is so. Hence, the up mentioned counter is increased when the severe hypoglycemia check is positive to prevent the blockage in this situation, in which the first version of the algorithm tended to be stuck.

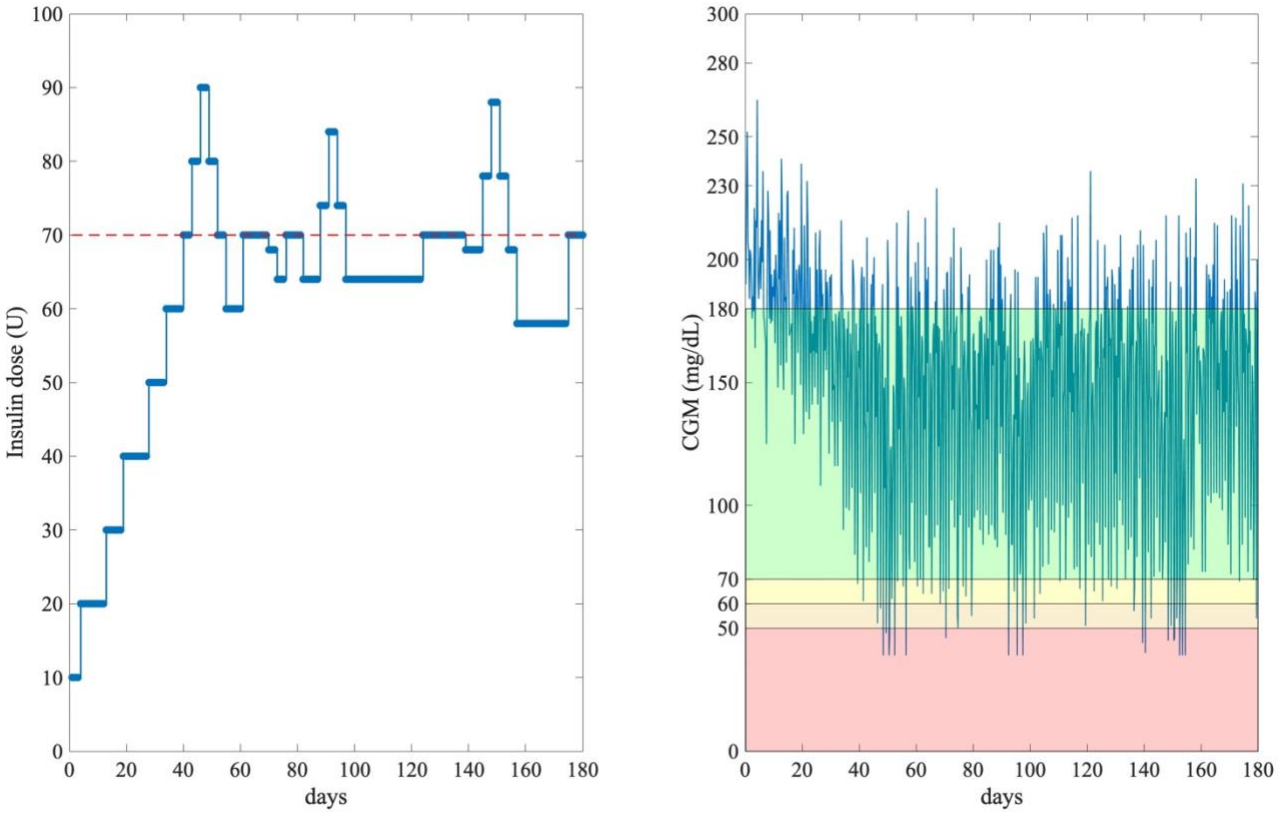

Figure 2.10 Insulin dose profile (left panel) administered by algorithm 1 during the first 180-days, in red dashed line the optimal basal-insulin dose. 180-days CGM (right panel) with the different ranges: in green it is represented the CGM target range (green), TH1associated CGM range (yellow), TH2 associated CGM range (orange), TSH associated CGM range (red).

As before for Algorithm 1, two cases depending on the value of *ExitFlag* are evaluated:

At the beginning, both flags (*ExitFlag and Back*) are setted to zero. Therefore as seen for *Algorithm 1*, it is asked to search a better basal-insulin dose. To do that, the algorithm tests if the subject is in eu- or hyperglycemia by using the TIR, and the following cases are considered:
:

- *The current measured TIR is the greatest obtained so far*

  In this case, when the subject TIR is improving no changes were made. Hence, the decision-making process and the struct of this part are unchanged to the respect of Algorithm 1.

- *The current TIR is not the greater obtained so far*

  In this case some changes were made with respect to *Algorithm 1*: when it proposes a previously administered dose because it is associated to a maximum TIR, the *Back flag* is set to one; thus, the algorithm interprets this event as the subject stopped his improvements phase.
  Therefore, if the previous maximum TIR is between 10% and 95%, the LT trend of the smoothed CGM is computed and interpolated by a first-order polynomial. Again, the p_1 is evaluated as the mean slope of the LT trend; the t-value is computes and the corresponding p-value is obtained.
  - If p_1*>0, pvalue<0.05*

    If the subject glycemia on average is still significantly raising, the algorithm proposes a 10 U incremented dose. Before administering the dose, it checks if the new dose is associated to previous severe hypoglycemic events: if the severe hypoglycemic check is positive, the increment is rejected, and *Back* is setted to one.
  - If p_1*>0, pvalue>0.05;* p_1*<0, pvalue>0.05*

    In these two cases the slope of the LT trend is not statistically significant, as in the previous version the current dose is kept.
  - If p_1*<0, pvalue<0.05*

    The slope of the interpolating polynomial is significantly negative; therefore, the subject is not improving anymore, and the 3-days CGM on average is descending. In this case, when the past maximum TIR is greater than 50% the associated dose is proposed as optimal (*ExitFlag* = 1) and the *Back* flag is setted to one

The steps used to manage hypoglycemic events remain the same of *Algorithm 1*:

- *TH1≥7.5%, TH2<5%, TSH<2.5%*

  The only change was made when the subject experiences a mild hypoglycemia, in fact when the algorithm looks back for the dose associated to a maximum TIR and assigns it to the subject, the *Back* flag is set to one.

- *ExitFlag* = 1

When the ExitFlag is setted to one by the algorithm the handling done is the same to the respect of the first version.

Finally, these changes brought more stability and limited the undesired behavior. This can be seen in the figure 2.11, where the same subject of the figure 2.10 was simulated in the same condition using the second version of the algorithm. As one can see, despite the first peak, the algorithm founds out as best dose 60 U, 10 U less then algorithm 1 and keeps it until the end of the in-silico trial, showing that the goal of more stability is achieved.

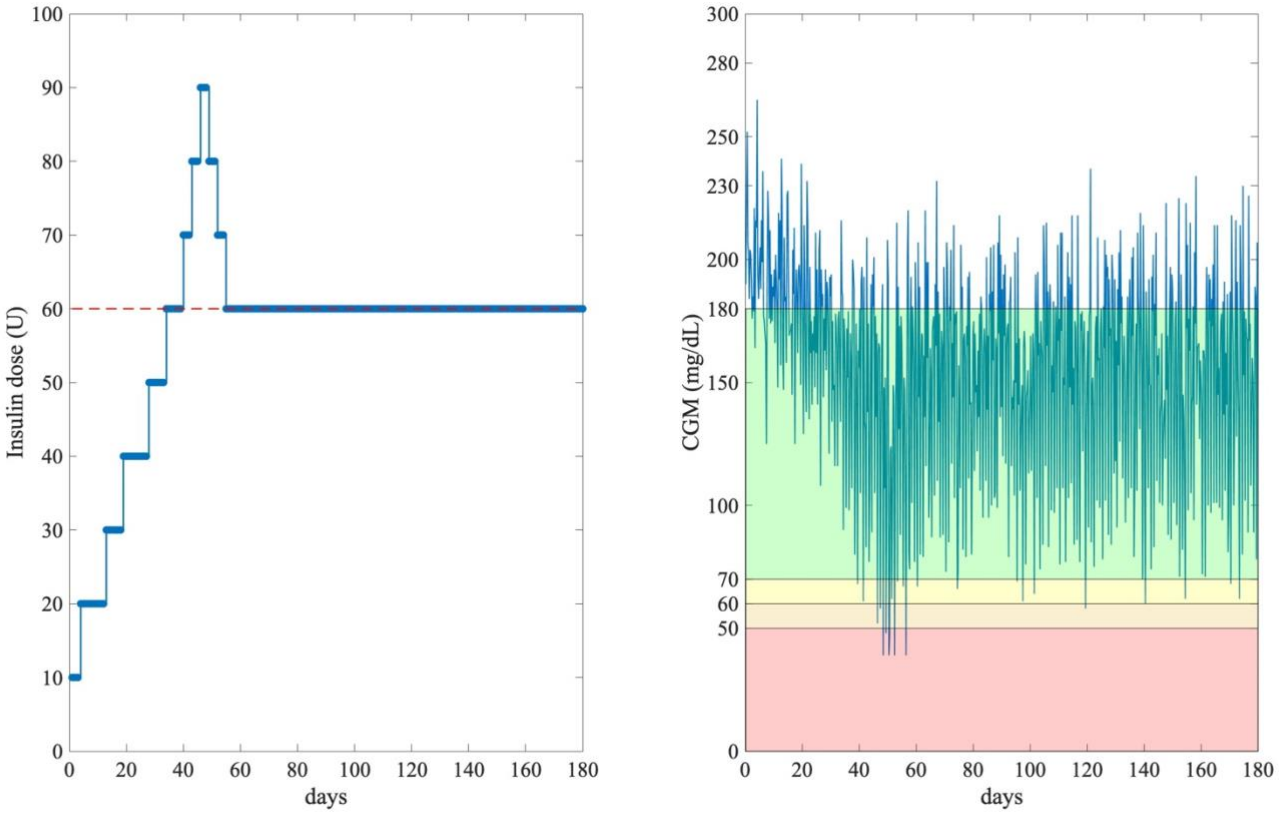

Figure 2.11 Insulin dose profile (left panel) administered by Algorithm 2 during the first 180-days, in red dashed line the optimal basal-insulin dose. 180-days CGM (right panel) with the different ranges: in green it is represented the CGM target range (green), TH1associated CGM range (yellow), TH2 associated CGM range (orange), TSH associated CGM range (red).

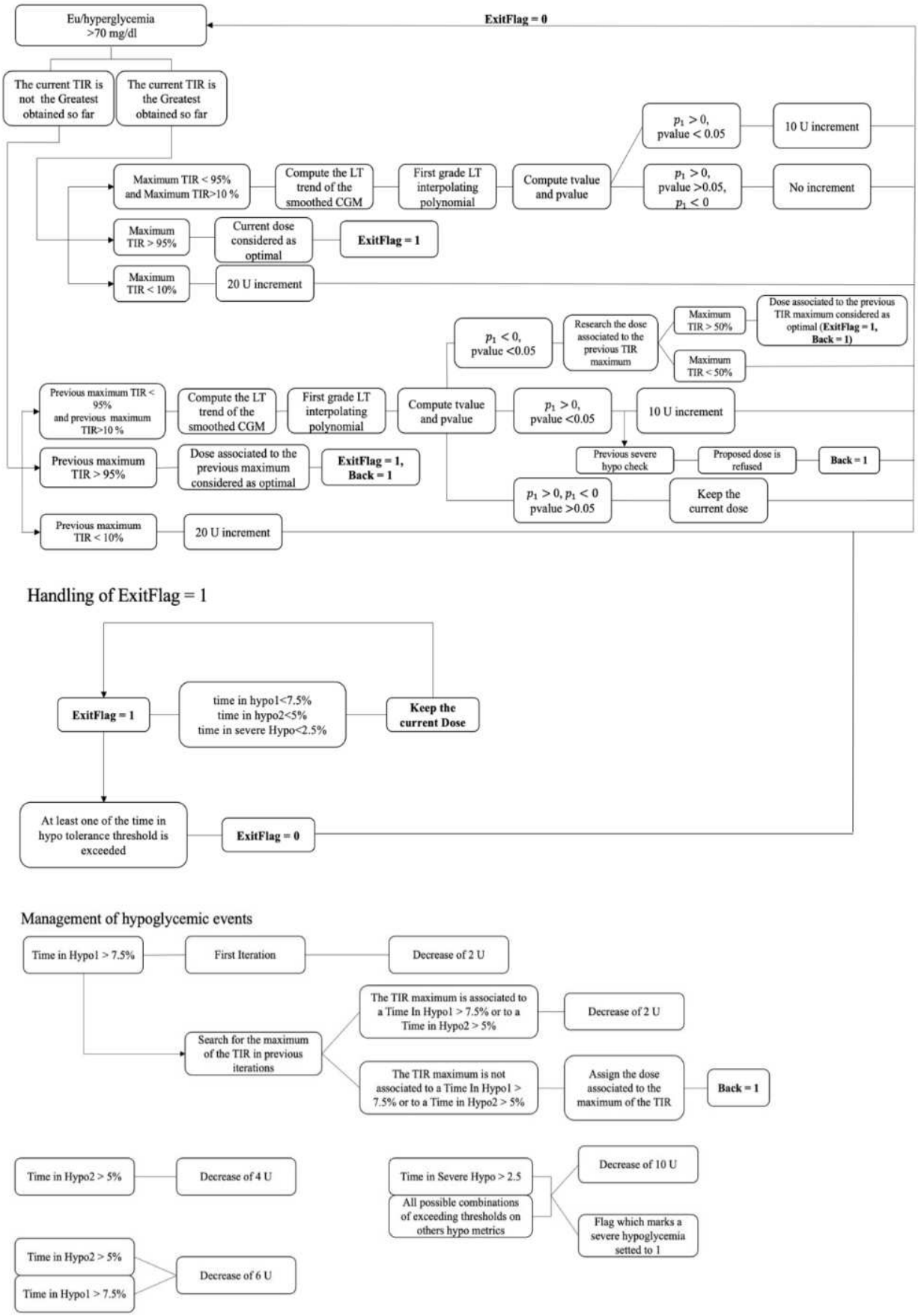

Figure 2.12 Flowchart of Algorithm 2, Eu/hyperglycemia management (above), handling of ExitFlag = 1 (middle) and management of hypoglycemic events (below)

2.5.2.4 Titration Algorithm 3

Once the stability was achieved by the changes done in the second version of the algorithm, now the focus was shifted to integrate new features that makes the algorithm more individualized. In particular, the previous two versions can administer only a rigid increment of 10 U, however it can occur that, both due to the subject characteristic or to the glycemic profile, the amount of the increment overcomes the actual insulin needs. Hence, a TIR proportional increment is needed.
Considering the generic iteration, different from the first, the mean 3-days TIR is used to determine the proportional increment. In fact, as previously said the TIR is characterized by 3 values associated to each day, which make up an iteration, here the average TIR of both the actual iteration (ATIR) and the previous one (PTIR) are used. Initially, two cases are considered:

- ATIR>PTIR

In this case, on average, TIR of the current iteration is greater to the previous one, hence the respective dose is considered. Therefore, for proposing a proportional increment a new bidimensional space is built, where the x-axis it has the mean values of the TIR, and y-axis has the values of insulin doses. Thus, a generic point of the space of the i-th iteration:

$$P_i = (ATIR_i, D_i) \qquad (2.37)$$

Where, $ATIR_i$ is the mean 3-days TIR and D_i is the correspondent insulin dose. Hence, when considering two consecutives iterations, there will be two points which defines univocally an interpolating first grade polynomial, which in this space will be defined as:

$$D = s_1 * TIR + s_2 \qquad (2.38)$$

This will be used for administering the proportional increment, in fact the information on which is built are based on the last 6 days. In figure 2.13 there is a graphical representation of the space and of the interpolating first grade polynomial described in *(2.38)*.

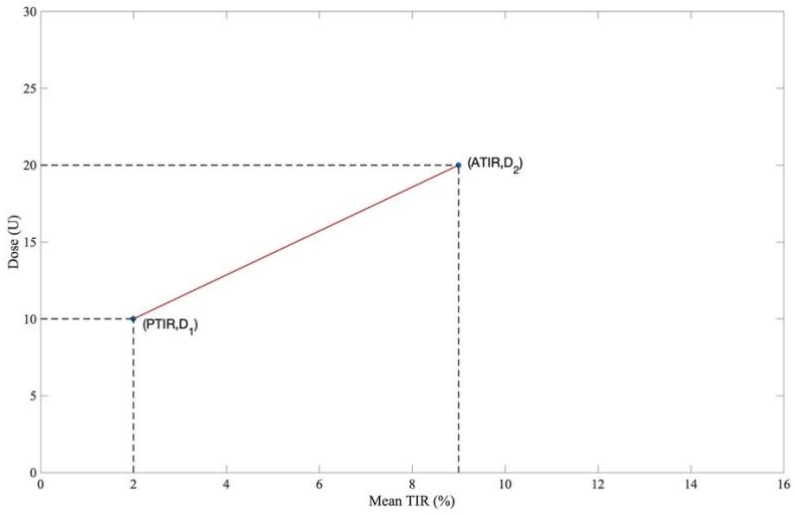

Figure 2.13 Cartesian axes used for obtaining the proportional increment. In blue the two points each relative to an iteration. The pedis 1 and 2 indicates the iteration

The information coming from ATIR and PTIR and the respective doses is used for the interpolation:

$$D_1 = s_1 * PTIR + s_2 \qquad (2.39)$$

$$D_2 = s_1 * ATIR + s_2 \qquad (2.40)$$

Once s_1 and s_2 are obtained from the information coming from the iterations, the target time in range (TTIR) can be defined as:

$$TTIR = ATIR + 5\% \qquad (2.41)$$

Since the minimum clinical relevant increment in TIR is 5%, by substituing TTIR in the *(2.38)* the dose at which the subject will have, theoretically, a 5% TIR increment is retrived. Thus, mathematically:

$$D_{inc} = s_1 * TTIR + s_2 \qquad (2.42)$$

Since TTIR can be computed, also D_{inc} can be easly calculated since s_1 and s_2 coefficients are the same calculated from the *(2.39)* and *(2.40)*. Once D_{inc} is known, the proportional dose increment (Propotional Increment) can be obtained:

$$Propotional\ Increment = D_{inc} - D_2 \qquad (2.43)$$

Depending on the two doses, $Propotional\ Increment$ (PI) can be both positive or negative, hence respectively $D_{inc} > D_2 \vee D_{inc} < D_2$. Therefore, the sign of this quantity is dictated by the insulin doses which depends by the mean values of the TIR. In the figure 2.14 a grafic representation of the proportional increment is presented.
Within the algorithm, different evaluations are performed in fact in the previous description was evaluated the case for granted that TTIR > PTIR, however the algorithm is built for condering also the opposite, this is fundamental when considering to build the x-axis. Furthermore, additional checks are implemented in order to limit the values of proportional increment: if s_1 is negative and PI is more negative than -10 U, since in this case the subject is not in hypoglycemia, the current dose is kept thus the decrement is discareded; if the PI is greater of 10 U, the dose is still incremented by 10 U for safety reason and finally if the PI is zero ($D_{inc} = D_2$) a 10 U increment is administered, this because this part is executed when the 3 days trend is significally raising. Ultimately, if PI overcomes all the checks, it is then summed to the current insulin dose and proposed to the subject.

- PTIR>ATIR

TIR achieved in the previous iteration is greater than the actual TIR, since the proportional increment is implemented when the LT trend of 3 days CGM is significally raising, this case is considered as a particular one. Hence, the a stardard 10 U increment is proposed to the subject.

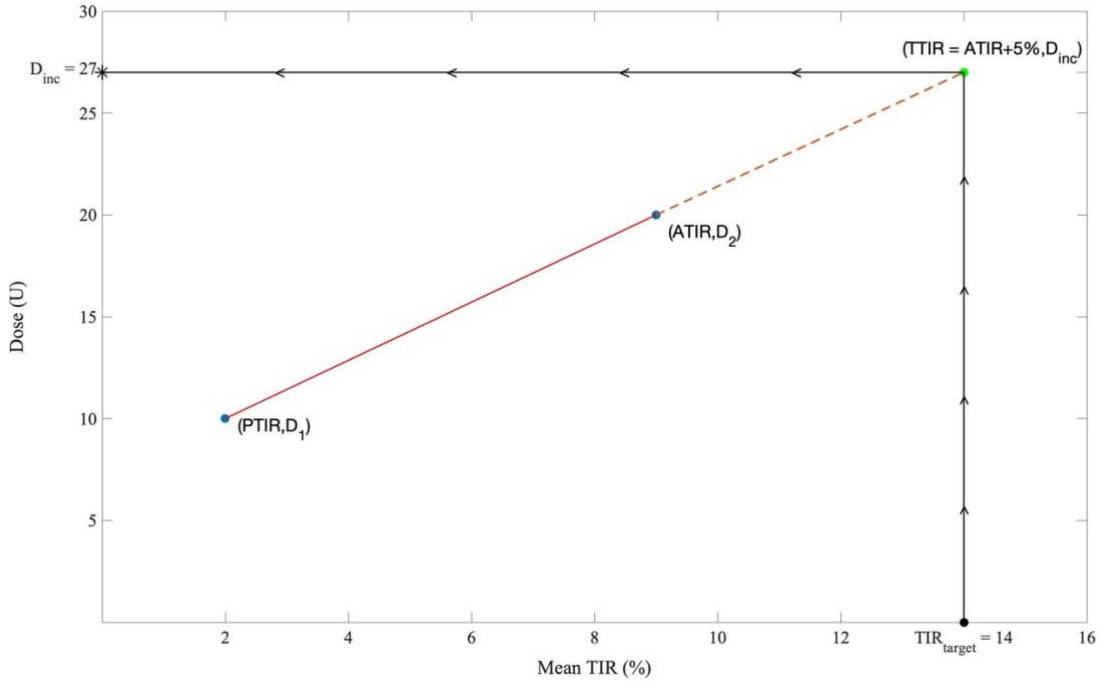

Figure 2.14 Proportional dose increment, the dashed line indicates the dose extrapolation corresponding to the TTIR of the interpolating polynomial defined by (PTIR, D_1) and (ATIR, D_2). The green point (TTIR, D_{inc}) defines the target point at which the TIR is incremented by 5%. The arrow on the black line indicates the direction of the PI operation, starting from the TTIR with the interpolating polynomial D_{inc} is obtained.

As for the previous two versions of the algorithm, Algorithm 3 is divided in two macroareas depending on the value of the *ExitFlag*:

At the beginning, *Exitflag* and *back are* set to zero

Thus, it means that the optimal Dose has not yet been found. Therefore, the algorithm is asked to search a better basal-insulin dose. To do that, first, then algorithm tests if the subject is in eu- or hyperglycemia. If this is the case, the subject did not exceed the hypoglycemic threshold already defined (i.e., TH1, TH2 and TSH). The TIR is calculated, and the following conditions may occur:

- *The current measured TIR is the greatest obtained so far*
  If 10%<TIR<95%, the LT trend of the smoothed CGM is computed and interpolated by a first-order polynomial. From *Eq 2.31,* the p_1 is evaluated as the mean slope of the LT trend. As discussed in *2.5.2.1,* the value of the t functional is computed (tvalue) and the corresponding p-value is obtained. This last is used for understanding if the p_1 estimate is statistically significant.
  - If $p_1>0$, *pvalue<0.05*

  In this case the average slope is significantly greater than zero, meaning that on average the LT trend based on 3-days CGM is raising. As results, the algorithm proportionally increments the dose. The procedure is described more in details above.

- If p_1>0, *pvalue>0.05;* p_1<0, *pvalue<0.05;* p_1<0, *pvalue>0.05*

  As previously seen, when the pvalue is greater than 0.05 the algorithm keeps the current dose, since the information are not statistically relevant. At the same time, when the mean slope is significantly lower than zero, the algorithm does not provide an increment because the subject glycemia, on average, is already descending.

- *The current TIR is not the greater obtained so far*

This portion of the algorithm was changed only in the case in which the TIR is between 10% and 95% and the interpolating polynomial of the LT trend has a slope that is significantly greater than zero (i.e., p_1>0, $pvalue$<0.05). Thus, when this happens the algorithm administers the proportional increment instead of the fixed one.

Finally, the management of hypoglycemic events and the handling of the subject glycemia when the *ExitFlag* is set to one by the algorithm are the same as the previous versions of the algorithm. In the figure the first 180 days simulated CGM, and dosing scheme are presented.

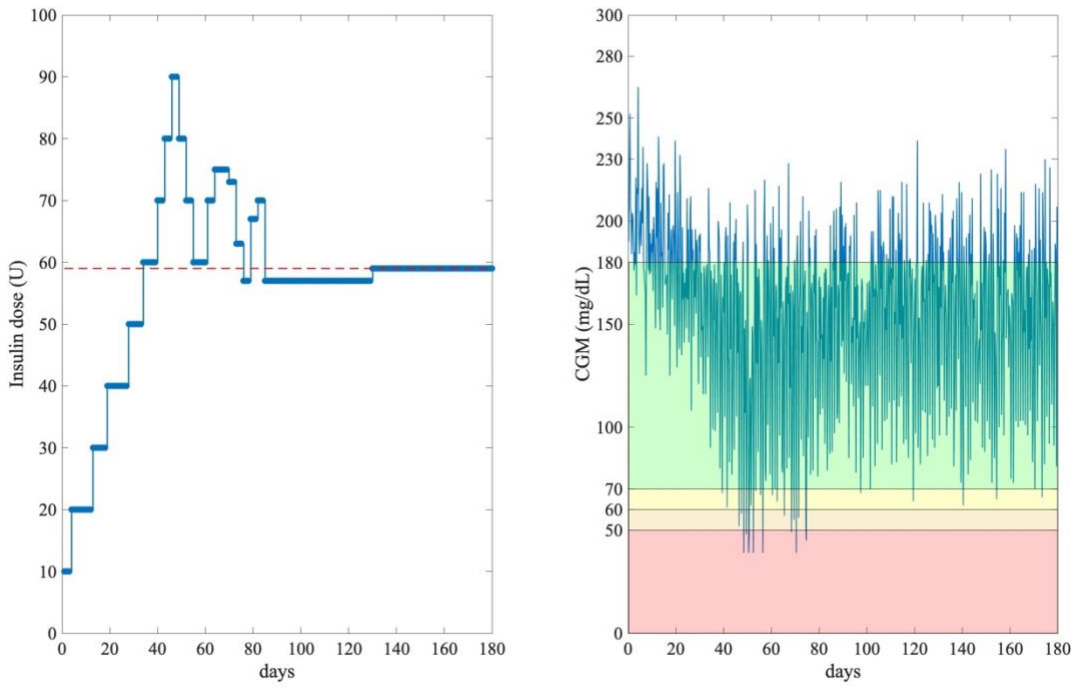

Figure 2.15 Insulin dose profile (left panel) administered by Algorithm 3 during the first 180-days, in red dashed line the optimal basal-insulin dose. 180-days CGM (right panel) with the different ranges: in green it is represented the CGM target range (green), TH1associated CGM range (yellow), TH2 associated CGM range (orange), TSH associated CGM range (red).

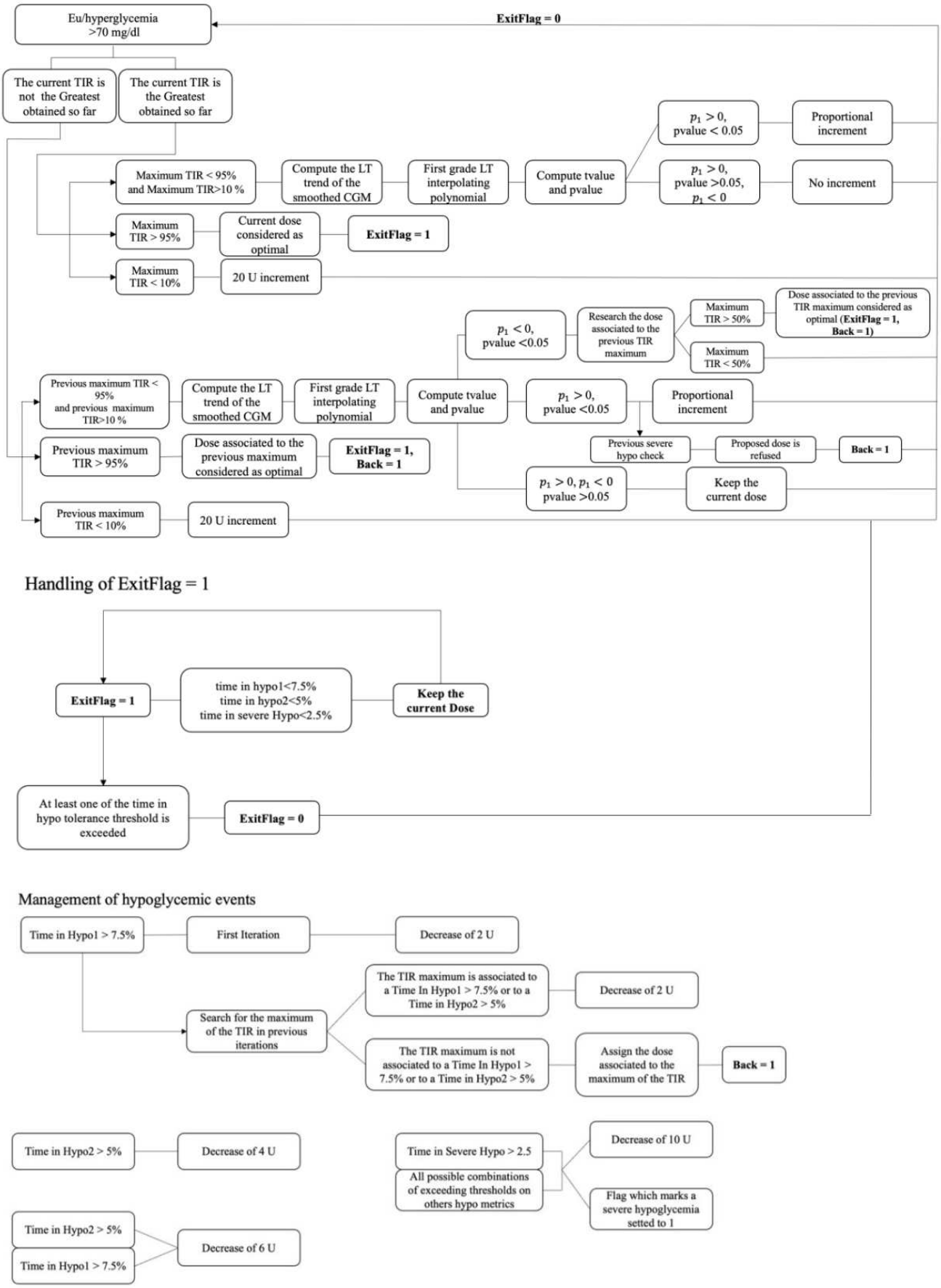

Figure 2.16 Flowchart of Algorithm 3, Eu/hyperglycemia management (above), handling of ExitFlag = 1 (middle) and management of hypoglycemic events (below)

2.5.2.5 Titration Algorithm 4

In this version, the attention was shifted on the behavior of the algorithm when the *ExitFlag* was set to 1. In the previous versions, there was an evaluation of the Hypoglycemic thresholds (i.e., TH1, TH2 and TSH), if one of them was exceeded the *ExitFlag* was setted to 0 and the algorithm restarted a new search by doing the sequence of operations extensively described previously. However, the reset to zero of the *ExitFlag*, especially when the dose was near to the optimal one, raises the probability of overshooting it or administering again a lower dose which raises the time that the subject spends above the glucose target.

At the beginning, *Exitflag* and *back are* set to zero

In this case, nothing was changed to the respect of the previous versions of the algorithm

- *ExitFlag* = 1

The handling was radically changed for the reason described above. In particular, it was inspired on the functioning of DUAL I. In fact, when the *ExitFlag* is set to 0 big steps are done towards the optimal dose until the *ExitFlag* is set to 1 by the algorithm. In the previous versions, when at least one of the hypoglycemic thresholds were exceeded, the *ExitFlag* was set to 0 again by the algorithm bringing it again into the eu/hyperglycemia loop. In this last version this possibility was eliminated:

- *TH1<7.5%, TH2<5%, TSH<2.5%*

  The optimal basal-insulin dose has been administered to the patient and there is not a significant hypoglycemic event, therefore the mean TIR on the 3 days is still computed:
  - *Mean TIR < 50%*

    In this case since the subject is not at risk for hypoglycemia, most of the time is spent above the glycemic target range. Thus, a 2 U increment is administered to try to lower the TAR
  - *Mean TIR > 50%*

    Also, the minimum time threshold for older/high-risk adult with type 2 diabetes[15] is achieved, hance the algorithm keeps the current dose and, as for the previous versions, it continues to monitor that the subject is not exceeding any of the hypoglycemic thresholds.

- *TH1>7.5%*

  This case is considered by the algorithm as a mild hypoglycemic case. Thus, to not exceed TH1 threshold again a 2 U decrement is administered

- *TH2 > 5%*

  When the TH2 threshold is exceeded, the algorithm detects a moderate hypoglycemic event, however still a 2 U increment is administered

- *TSH>2.5%*

  In this situation, despite the flag was setted to one by the algorithm, a severe hypoglycemic event has occurred, this can happen due to variation in the physical activity coupled with a reduced carbohydrate intake. However, a 4 U decrement is administered to reduce the time spent below the 50 mg/dL.

In figure 2.17 a representation of possible dosing scheme which shows the big steps done when the *ExitFlag* is setted to zero, and finer movement done when the *ExitFlag* value is equal to 1.

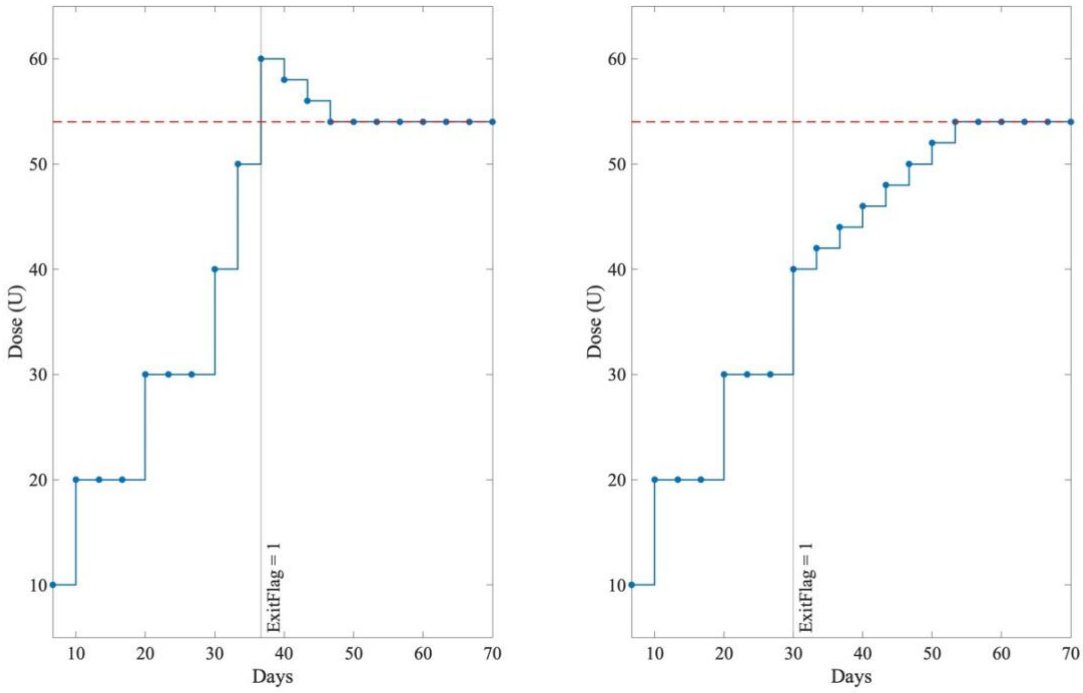

Figure 2.17 Two Possible situations after which the ExitFlag was set to one: on the left, an overshoot of the optimal dose (54 U) with the gradual descend, on the right the gradual increment done when the mean TIR is lower than 50%. The black vertical line marks the time from which the ExitFlag is equal to 1.

Finally, as for the other versions of the algorithm the 180 days simulated CGM and the dosing scheme of subject 39 are showed.

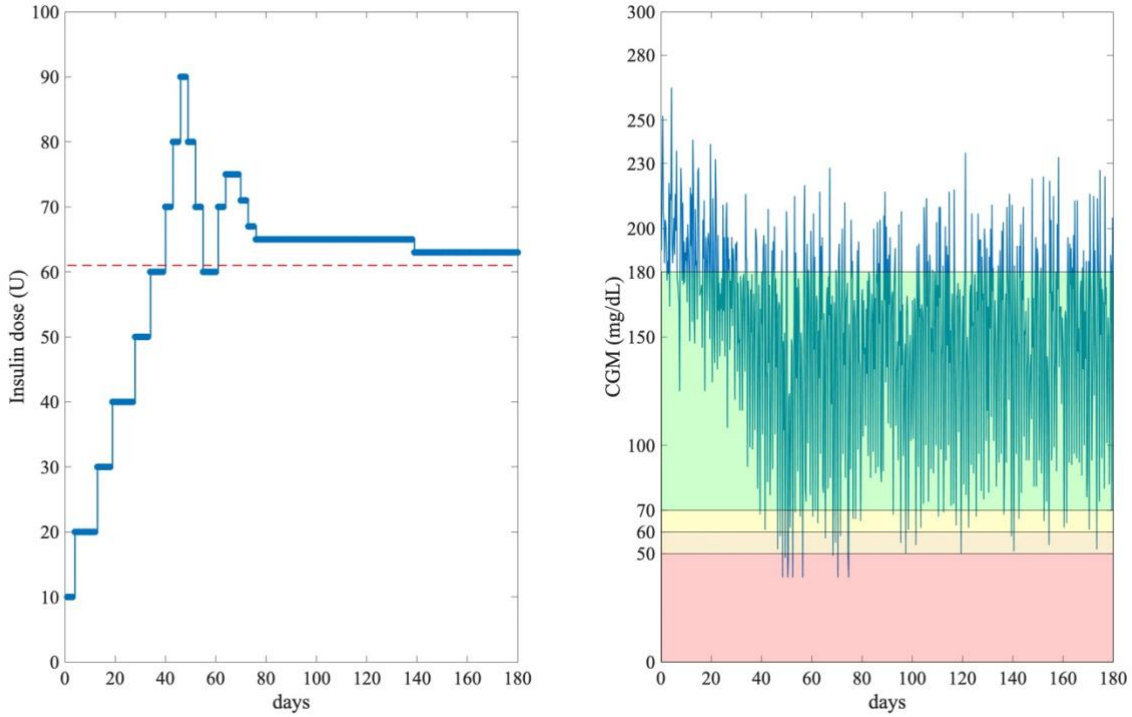

Figure 2.18 Insulin dose profile (left panel) administered by Algorithm 4 during the first 180-days, in red dashed line the optimal basal-insulin dose. 180-days CGM (right panel) with the different ranges: in green it is represented the CGM target range (green), TH1associated CGM range (yellow), TH2 associated CGM range (orange), TSH associated CGM range (red).

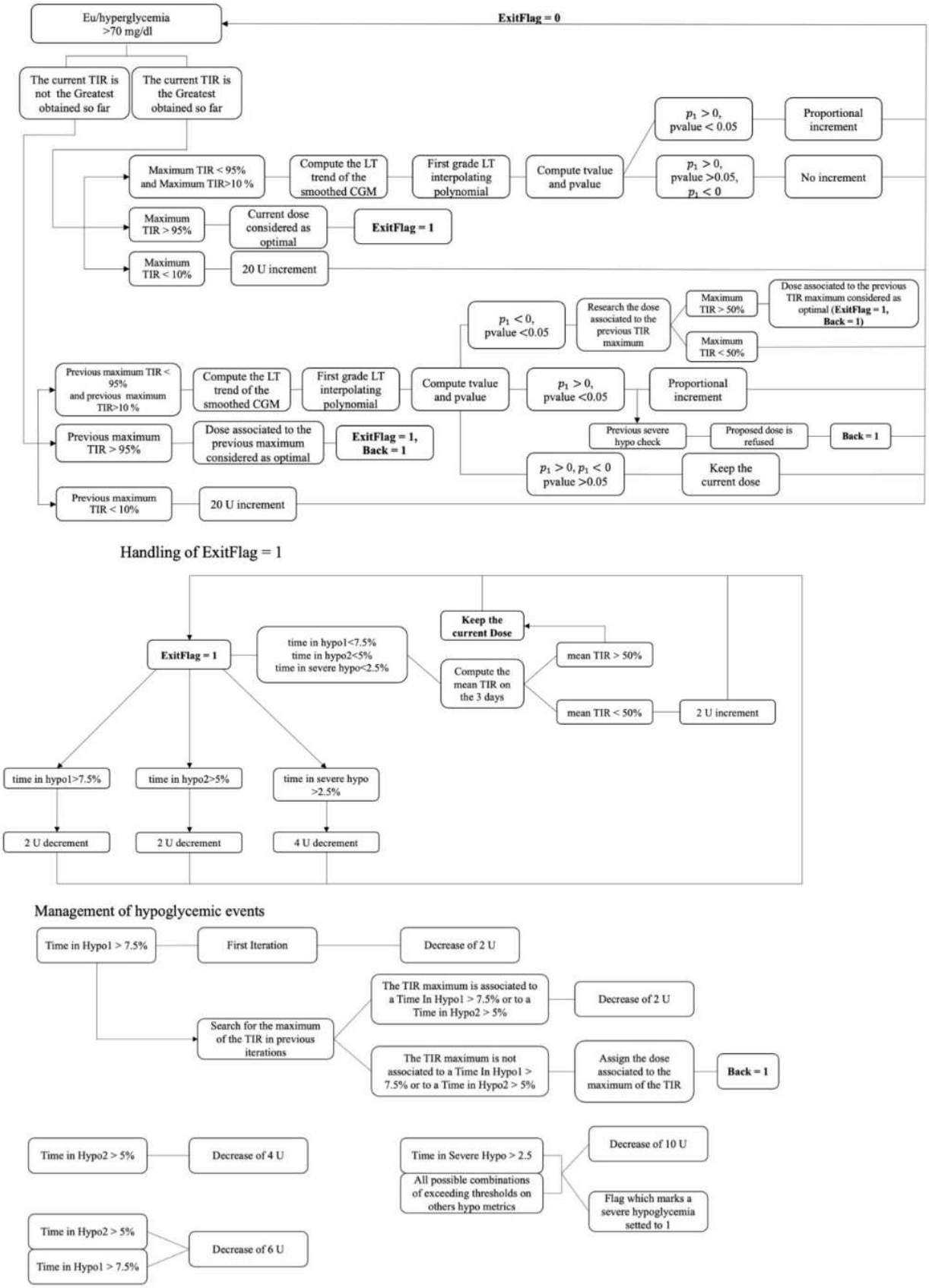

Figure 2.19 Flowchart of Algorithm 4, Eu/hyperglycemia management (above), handling of ExitFlag = 1 (middle) and management of hypoglycemic events (below)

2.5 Statistical and Clinical analysis

In this section, the statistical tests used to compare the new algorithms, in terms of CGM-time metrics, optimal dose and FPG, and the DUAL I are reported.
First, it is fundamental to assess whether the distribution of the considered metric is normally distributed or not. To do this, the Shapiro-Wilk test[39] is used, which uses two variance estimators:

- A non-parametric statistic estimator based on the linear combination of the rank order of a random variable.
- A parametric variance estimator which provides the sample variance.

These two statistical estimators are used for building the functional W:

$$W = \frac{\left(\sum_{i=1}^{n} a_i x_{(i)}\right)^2}{\sum_{i=1}^{n}(x_i - \bar{x})^2} \qquad (2.44)$$

Where $x_{(i)}$ is the i-th smallest sample value, hence the rank I. Moreover, $\bar{x}$ is the sample arithmetic mean:

$$\bar{x} = \frac{x_1 + \cdots + x_n}{n} \qquad (2.45)$$

The constants a_i are defined as:

$$(a_1, \ldots, a_n) = \frac{m^T V^{-1}}{(m^T V^{-1} V^{-1} m)^{\frac{1}{2}}} \qquad (2.46)$$

The vector m is defined as:

$$m = (m_1, \ldots, m_n)^T \qquad (2.47)$$

where $m_1, \ldots, m_n$ are the expected values of the ranks and V it is the ranks covariance matrix. By definition, the functional W can assume value between 0 and 1 and it is used to the test the normality of parameter distributions. Thus, if the test is not able to refuse the null hypothesis the samples value (i.e., the CGM metrics distribution) are normally distributed, vice versa they are not.
The Shapiro-Wilk test is applied to each CGM time metric (TIR, TAR and TBR) and on FPG. As discussed in section 2.4, the test was done on the HIN classified subject.
In the results section this test is first used and then, if the metrics are normally distributed, they are be represented as:

$$\overline{metric} \pm \sigma_{metric} \qquad (2.48)$$

Where, $\overline{metric}$ is the mean value of the generic CGM time metric and σ_{metric} is the relative SD. Meanwhile, if the metrics are not normally distributed, they will be showed as:

$$\widetilde{metric} \ \& \ IQR_{metric} \qquad (2.49)$$

In which, $\widetilde{metric}$ is the median of the generic CGM time metric and IQR_{metric} is the associated IQR. Furthermore, assessing if the distribution of the metrics is normal or not is fundamental for choosing the right test to assess whether 2 different algorithms provide results which are statistically different. In fact, if the metrics are normally distributed the paired two-tailed t-test[40] is used:

$$\begin{cases} H_0: \ \mu_d = 0 \\ H_1: \ \mu_d \neq 0 \end{cases} \qquad (2.50)$$

Where, μ_d is the true mean difference. On the other hand, if the data are not normally distributed the Mann-Whitney U-test[41] for paired data is applied on the CGM metric sample to find median differences:

$$\begin{cases} H_0: \ m_1 = m_2 \\ H_1: \ m_1 \neq m_2 \end{cases} \qquad (2.51)$$

Where m_1 and m_2 are the median of two CGM time metrics associated to the specific titration rule. However, a fundamental step is choosing the algorithm with the best performances. For normally distributed metrics the F-test in one-way analysis of variance (ANOVA) is performed on CGM metrics. It is used to assess whether the expected values of a quantitative variable within several pre-defined groups differ from each other. The ANOVA test is based on the F-test statistic, which for this purpose is formulated as follows:

$$F = \frac{explained \ variance}{unexplained \ variance} = \frac{between - group \ variability}{within - group \ variability} \qquad (2.52)$$

Generally, the ANOVA tests if the means of a certain number of groups are significant different. Thus, the null hypothesis (H_0) in the comparison regards if the means of the groups are all the same, however, the alternative hypothesis (H_1) typically is formulated for assessing if at least one of the groups mean is different. The ANOVA test was applied to each normally distributed metric produced by the algorithms. Hence, it was used for finding differences between the 4 means of the metrics compared at 4 different cumulative time checkpoints (i.e., third, sixth, nineth, twelfth month).
For non-normally distributed metrics the Kruskal-Wallis test[42] is used. It is a non-parametric version of the one-way ANOVA based on the extension of the Mann-Whitney U test to more than 2 groups, thus the data are pooled and ranked from the smallest to the largest, then the sums of ranks in each subgroup are added up, and the probability is calculated. The statistic H is defined as follows:

$$H = (N-1)\frac{\sum_{i=1}^{g} n_i(\bar{r}_i - \bar{r})^2}{\sum_{i=1}^{g}\sum_{j=1}^{n_i}\left(r_{ij} - \bar{r}\right)^2} \qquad (2.53)$$

Where, n_g is the number of observations in the group g, r_{ij} is the rank of the observation j within the group i, N are the observations of all groups and $\bar{r}_i$ is defined as follows:

$$\bar{r}_i = \frac{\sum_{j=1}^{n_i} r_{ij}}{n_i} \qquad (2.54)$$

Moreover, beyond the statistical tests used for inferring information on the metric distributions and on metric differences which can occur due to the application of different titration protocol, also some clinical assessment should be taken in consideration. Despite differences in the population regarding the possibility of reaching standardized CGM time metric target values, there are guidelines to assess the efficacy of glycemic control for adult and/or older/high-risk T2D patient[16].
In particular, TIR needs to be above 70%, i.e., 16 hours and 48 minute per day spent in the glycemic target range, while for the Older/high-risk subject the TIR lower boundary is equal to 50%, hence at least 12 hours must be spent by the subject within the glycemic target. For the two up mentioned categories, 5% is the clinically relevant TIR improvement since this increment brings clinically significant benefits to the patient.
Concerning TBR, it is fundamental to stick it as much as possible to the guides provided by the international consensus. The percentage of the reading for standard T2D patient should be less than 4% (i.e., less than 1 hour) when considering values lower than 70 mg/dL, while for older/high-risk subjects the percentage drops to 1% or equivalently less than 15 min spent daily below the target glycemic range. Meanwhile, in the case of the TAR, the percentage of CGM samples acquired should be less than 25% (i.e., less than 6 hours) spent above 180 mg/dL and less than 5% (<1 hour and 12 minutes) above 250 mg/dL. For older/high-risk categories just the percentage of samples time which lay above 250 mg/dL is defined and it should be less than 10% (i.e., <2 hours and 24 minutes). In figure 2.20, a visual representation of the CGM time target along with the time metrics is shown.

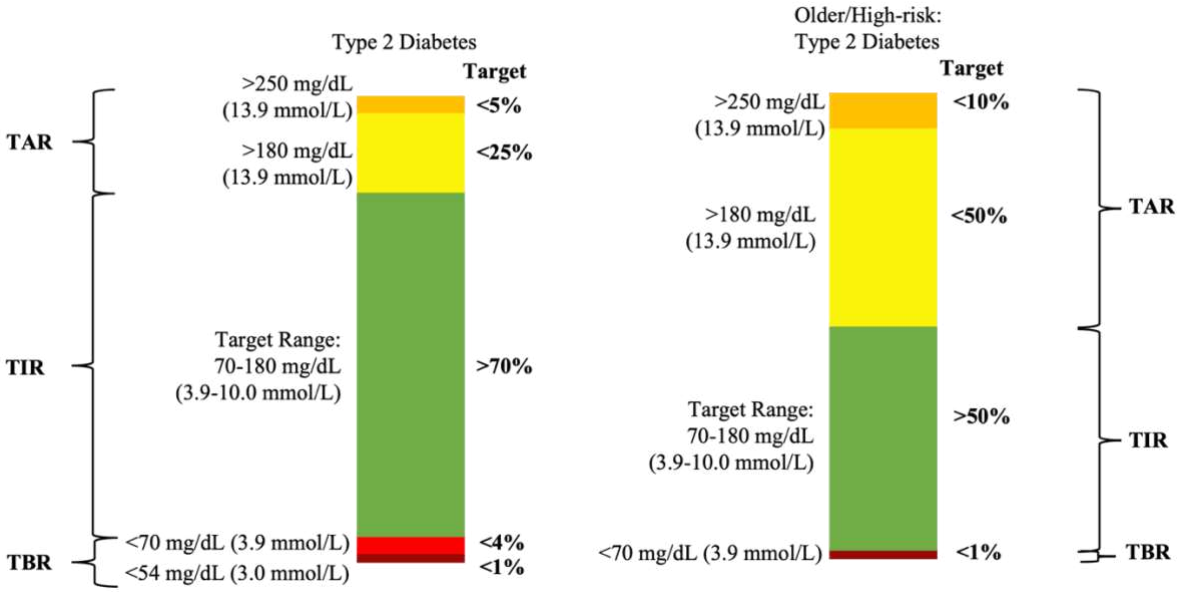

Figure 2.20 CGM-based target for T2D subject (left) and for older/High-risk patients (right). Adapted from [16]

Finally, the best algorithm is selected after comparing the different metrics at each time points using the ANOVA or Kruskal-Wallis tests, furthermore a posteriori analysis is done. In fact, for each algorithm the Pearson correlation (ρ) and the coefficient of determination (R^2) are computed using the HIN subject final doses of DUAL I and of the specific algorithm. Thus, the Pearson correlation measures the strength of the linear relationship between 2 variables. Let OID_{DUALI} be the final doses computed by DUAL I and $OID_{Algorithmx}$ that provided by the algorithm x where x is the version:

$$\rho = \frac{cov\left(OID_{DUALI}, OID_{Algorithmx}\right)}{\sigma_{FD_{DUALI}}\sigma_{FD_{Algorithmx}}} \quad (2.55)$$

Where, cov is the covariance operator and σ is the SD. The algorithm that has the higher correlation with DUAL I will be considered as the best one. In fact, this means that the best version of the algorithm administers a dose which will be linearly correlated with the one provided by DUAL I, therefore the major difference lays in the time used for administering the optimal dose and not in the dose itself.

This is a fundamental step in basal-insulin titration algorithm, in fact, lowering the titration time will result in less time spent above the glycemic target and in an increase of TIR. Furthermore, if the final dose is correlated to the one administered by DUAL I, the FPG relative to the new algorithm should match the clinical boundaries (even if this metric is not considered at implementation level for the new algorithms). Hence, even if the new CGM-based approaches do not consider the subject fasting glucose, which is used and clinically accepted, they are still able to bring this value within safety ranges.

Moreover, to further understand the relationship occurring between the 2 final dose sets also a simple linear regression is performed, from which the R^2 statistic was extracted and evaluated, beyond the analysis done on the correlation. In fact, the R^2 indicates the proportion of variance in the dependent variable (i.e., algorithm x final doses) that can be explained by the independent variable (i.e., DUAL I final doses). It can be defined as:

$$R^2 = 1 - \frac{SSR}{SST} = 1 - \frac{\sum(y_i - \hat{y}_i)^2}{\sum(y_i - \bar{y}_i)^2} \quad (2.56)$$

SSR is the residual sum of squares, where y_i is the actual value of y while $\hat{y}_i$ is the predicted value. SST is the total sum of squares which is squared the sum of the distance between the data and the mean (i.e., $\bar{y}_i$).

CHAPTER 3

Results

3.1 Best Titration Algorithm Selection

In this section, the new algorithms are compared using the statistical tests described in section 2.5, and this was done to determine the best one in terms of performance and similarity with DUAL I. The first step was to evaluate the normality of the distributions (Tables 3.1, 3.2, 3.3, 3.4 and 3.5) and then the proper test was used to investigate possible statistical differences among them (tables 3.6, 3.7, 3.8 and 3.9). In most cases the TIR are normally distributed, as well as for the TAR and the FPG. However, the TBR is never normally distributed. Also, the FPG relative to the first month checkpoint is never normally distributed, this can be because algorithms require more time to uniform the fasting glucose of HIN subjects. Finally, the DUAL I rule provides metrics which are not normally distributed at all cumulative time checkpoints.

Algorithm 1 Time Metric	1 month	3 months	6 months	9 months	12 months
TIR	0.89	0.59	0.87	0.85	0.74
TAR	0.89	0.27	0.48	0.62	0.51
TBR	$1.76 * 10^{-11}$	$2.55 * 10^{-7}$	$3.49 * 10^{-7}$	$3.33 * 10^{-7}$	$3.29 * 10^{-7}$
FPG	0.05	0.19	0.51	0.62	0.30

Table 3.1 Algorithm 1 p-values of the Shapiro-Wilk test.

Algorithm 2 Time Metric	1 month	3 months	6 months	9 months	12 months
TIR	0.89	0.17	0.04	0.04	0.04
TAR	0.89	0.08	0.02	0.03	0.03
TBR	$1.76 * 10^{-11}$	$2.67 * 10^{-7}$	$3.55 * 10^{-7}$	$4.21 * 10^{-7}$	$3.51 * 10^{-7}$
FPG	0.05	0.38	0.66	0.69	0.66

Table 3.2 Algorithm 2 p-values of the Shapiro-Wilk test.

Algorithm 3 Time Metric	1 month	3 months	6 months	9 months	12 months
TIR	0.89	0.95	0.97	0.88	0.85
TAR	0.89	0.78	0.94	0.77	0.72
TBR	$4.84 * 10^{-12}$	$5.39 * 10^{-8}$	$2.33 * 10^{-7}$	$3.15 * 10^{-7}$	$5.55 * 10^{-7}$
FPG	0.02	0.64	0.92	0.27	0.64

Table 3.3 Algorithm 3 p-values of the Shapiro-Wilk test.

Algorithm 4 Time Metric	1 month	3 months	6 months	9 months	12 months
TIR	0.89	0.95	0.99	0.91	0.84
TAR	0.89	0.74	0.99	0.80	0.57
TBR	$4.84 * 10^{-12}$	$2.69 * 10^{-8}$	$3.46 * 10^{-7}$	$1.08 * 10^{-6}$	$3.63 * 10^{-6}$
FPG	0.02	0.79	0.79	0.07	0.63

Table 3.4 Algorithm 4 p-values of the Shapiro-Wilk test.

DUAL I Time Metric	1 month	3 months	6 months	9 months	12 months
TIR	$3.84 * 10^{-8}$	$3.85 * 10^{-8}$	$6.79 * 10^{-7}$	$2.10 * 10^{-5}$	$2.66 * 10^{-5}$
TAR	$3.75 * 10^{-8}$	$1.83 * 10^{-8}$	$2.61 * 10^{-7}$	$8.81 * 10^{-6}$	$1.45 * 10^{-5}$
TBR	0	0	0	0	0
FPG	0.01	$4.09 * 10^{-9}$	$4.56 * 10^{-10}$	$2.52 * 10^{-8}$	$6.45 * 10^{-9}$

Table 3.5 DUAL I p-values of the Shapiro-Wilk test

Subsequently, the ANOVA test was employed to compare each CGM-time metric among the 4 new Algorithm. The results of the ANOVA test can be found in tables 3.6, 3.7, 3.8, and 3.9, which display the two-group comparisons alongside the corresponding p-values.

TIR ANOVA test					
Algorithm i	*Algorithm j*	***3rd month***	***6th month***	***9th month***	***12th month***
1	*2*	1	1	1	1
1	*3*	1	1	0.96	0.97
1	*4*	1	0.99	0.96	0.96
2	*3*	1	0.98	0.91	0.91
2	*4*	1	0.97	0.89	0.89
3	*4*	1	1	1	1

Table 3.6 TIR ANOVA test p-values after 3rd, 6th, 9th and 12th months.

TAR ANOVA test					
Algorithm i	*Algorithm j*	***3rd month***	***6th month***	***9th month***	***12th month***
1	*2*	1	1	1	0.99
1	*3*	1	1	1	1
1	*4*	1	1	1	1
2	*3*	1	1	1	0.95
2	*4*	1	1	0.99	0.94
3	*4*	1	1	1	1

Table 3.7 TAR ANOVA test p-values after 3rd, 6th, 9th and 12th months.

TBR Kruskal-Wallis test					
Algorithm i	*Algorithm j*	***3rd month***	***6th month***	***9th month***	***12th month***
1	*2*	1	0.98	0.97	0.89
1	*3*	0.91	0.65	0.36	0.31
1	*4*	0.91	0.77	0.32	0.25
2	*3*	0.91	0.86	0.62	0.74
2	*4*	0.91	0.93	0.58	0.68
3	*4*	1	0.99	1	0.99

Table 3.8 TBR Kruskal-Wallis test p-values after 3rd, 6th, 9th and 12th months.

FPG ANOVA test					
Algorithm i	*Algorithm j*	***3rd month***	***6th month***	***9th month***	***12th month***
1	*2*	1	0.94	0.98	0.98
1	*3*	0.97	1	1	1
1	*4*	0.98	0.98	1	1
2	*3*	0.99	0.96	0.98	0.99
2	*4*	1	1	0.98	0.98
3	*4*	1	1	1	1

Table 3 FPG ANOVA test p-values after 3rd, 6th, 9th and 12th months.

In the figure 3.1, TIR, TAR, TBR and FPG are reported for each of the new Algorithms.

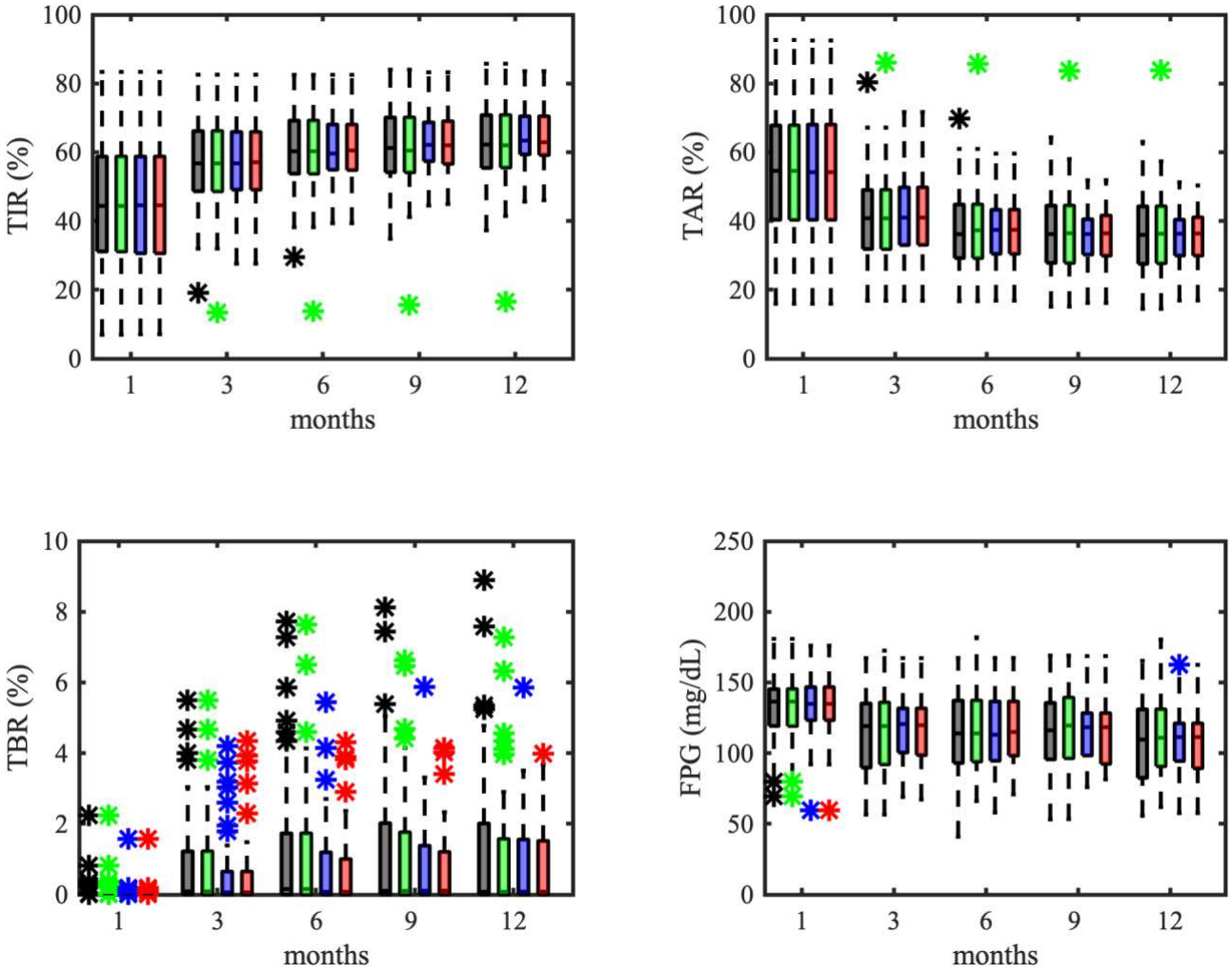

Figure 3.1 Time metrics of the different versions of the algorithm: Algorithm 1 (gray), Algorithm 2 (green), Algorithm 3 (blue) and Algorithm 4 (red); The metric showed are the TIR (upper left panel), the TAR (upper right panel), the TBR (lower left panel) and FPG (lower right panel).

Despite the absence of statistical differences among CGM metrics between the different versions of the Algorithm, some conclusions regarding the best one can still be outlined. Visually, the last two versions of the Algorithm show the absence of outliers at 3-,6-, and 12-month in TIR, coherently they are not present also in the TAR metric. Moreover, for the TIR, the TAR and the FPG, the last 2 versions of the Algorithm have narrower boxplot, meaning that the metric has a lower IQR. However, the last version of the Algorithm does not exceed the 4 % tolerance boundaries on the TBR. Hence, also this criterion suggests that Algorithm 4 is the best among the other versions.
Furthermore, when considering the mean dose computed on the population for the whole in-silico trial duration (see figure 3.2), one can see that the last version of the Algorithm is not the faster in up-titrating subjects (table 3.10), but on average the optimal dose is achieved after 61 days, which is still way less than the half of the mean time that DUAL I needs for administer its optimal dose.

Titration rule	*Mean Time for administering the optimal dose (days)*
DUAL I	151 (max = 187, min = 49)
Algorithm 1	43 (max = 46, min = 28)
Algorithm 2	40 (max = 43, min =28)
Algorithm 3	64 (max = 112, min = 22)
Algorithm 4	61 (max = 67, min =22)

Table 3.10 Mean, maximum and minimum time for administering the optimal dose in each new algorithm.

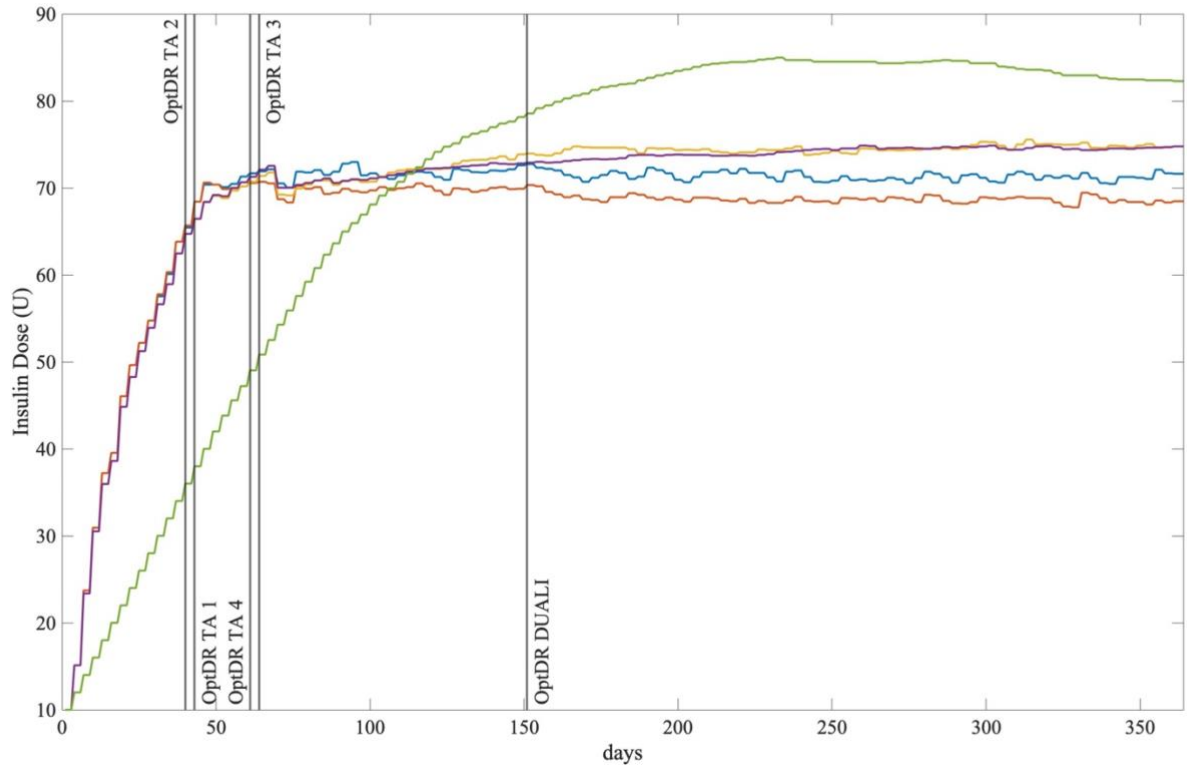

Figure 3.2 The lines are the mean dose computed on the population considering the whole 52-week in-silico trial: DUAL I in green, Titration Algorithm 1 (TA1) in blue, Titration Algorithm 2 (TA2) in red, Titration Algorithm 3 (TA3) in yellow and Titration Algorithm 4 (TA4) in violet. The vertical black line indicates on average the amount of time needed by each algorithm for administering the relative optimal insulin dose.

Finally, another difference between the *Algorithm 4* and the other versions obtained from the figure 3.2 is the smoothness: the last version of the Algorithm is much smoother and flat when considering the pathways after the mean convergence time; meaning that, on average, the fourth version of the Algorithm is the most stable, i.e. it avoids administering abrupt dose changing which can be caused by daily fluctuation of the subject glycemia.

Finally, the optimal end doses of each Algorithm are compared with those obtained with DUAL I in terms of correlation and R^2. In figure 3.3, different scatter plots with the regression line for all the different versions of the Algorithm are reported.

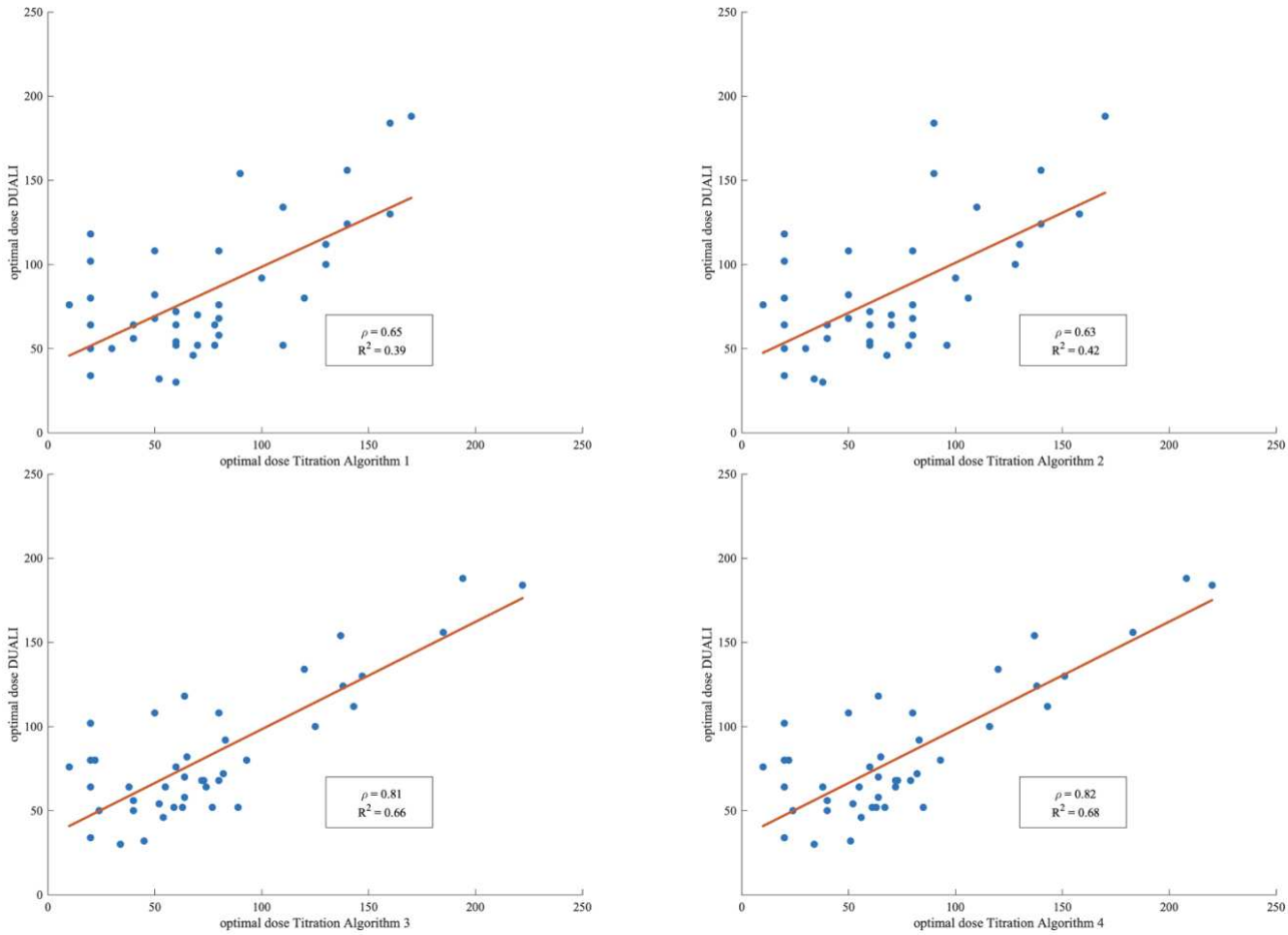

Figure 3.3 Scatter plots of optimal insulin dose of DUAL I vs. Algorithm 1 (left higher panel), Algorithm 2 (right higher panel), Algorithm 3 (left lower panel) and Algorithm 4 (right lower panel). In red the linear regression lines. In the box the linear correlation coefficient (ρ) and the coefficient of determination (R^2) are showed

In conclusion, as one can immediately see through the different versions of the Algorithm, there is a clear improvement in the R^2 statistic, starting from 0.39 is almost doubled (0.68) in the last version of the Algorithm meaning that the linear relationship between the final DUAL I doses, and the optimal Algorithm 4 doses has significantly improved. This is also supported by the progress made in the linear correlation. In fact, there is a remarkable improvement when considering the first two versions of the Algorithm and the third one (i.e., from 0.65/0.63 to 0.81), as well as a smaller improvement going from the third to the fourth version (i.e., from 0.81 to 0.82). Regarding these results the last version of the Algorithm was chosen with this criterion.

In the end, for all the reasons presented above and accordingly to the various criteria mentioned, *Algorithm* 4 is considered as the best algorithm among the others. The results achieved will be presented and compared to the ones provided by DUAL I in section 3.2 of this work.

3.2 Best Titration Algorithm vs DUAL I

In this section, the best algorithm selected in section 3.1 (i.e., *Algorithm 4*) is compared with the state of the art of the basal-insulin titration rule, thus, DUAL I. For understanding possible differences which can occur within the cohort of T2D patient, the metrics are evaluated until the first, third, sixth, nineth and twelfth month; hence, each CGM-time metric and the FPG will be presented and evaluated (figure 3.4).

First, one can immediately see that statistical differences are found in the first and third months for the TIR and the TBR, for the TAR statistical differences are also found at the sixth month, while, for the FPG, the difference is statistically significant only at the first month.

Regarding the statistical difference at the first month in TIR, *Algorithm 4* achieved a median TIR of 44%, while DUAL I 36%. As previously said the minimum increase in the TIR which could lead to clinical relevant improvement is 5%[16]: *Algorithm 4* was able to almost double this value within the first month; furthermore, the IQR is lower (28% for the Algorithm 4 vs. 39% provided by DUAL I). Thus, when applying a faster titration rule such as *Algorithm 4*, TIR value results more bunched up around the median. Hence, limiting possible variations in the population response to basal-insulin titration rules, that can occur due to inter- and intra-variability allows to better stick to clinical CGM target; this tendency to have much lower IQR values is preserved through until the last time cumulative checkpoint (i.e., twelfth month). The difference is maintained also at the third month (Algorithm 4 showed a median TIR of 57% and DUAL I of 48%). Hence, not only the almost doubled clinically significant difference with DUAL I is preserved, but using *Algorithm 4* for 2 more months leads to a TIR improvement of 13 %. The sixth, nineth and twelfth comparisons were not statistically significant.

For what concerns the TBR, in figure 28 the 4 % tolerance threshold used in the clinical practice is highlighted. As for the TIR, statistical differences are found only in the first and third months. Especially, when considering the first month, median values for both *Algorithm 4* and DUAL I were zero, despite this the Mann-Whitney test indicates a statistical difference. Moving to the third month, the last version of the Algorithm performs slightly worse with respect to DUAL I, in median within 3 months subjects spend 0.06% below 70 mg/dL. However, there are several outliers which lays near the tolerance threshold without going above it. In general, up-titrated subjects using the *Algorithm 4* have an overall higher probability of experimenting hypoglycemic event: more aggressive rules tend to arrive faster to the target (i.e., normalize the glycemia of the subject), but the likelihood of overshooting the target is higher. Despite this, the TBR differences are not statistically significant when considering sixth, nineth and twelfth month assessments.

The TAR metric is the one that provides the greater improvement. As already discussed in the introduction, spending time above the glycemic target raises the risk of experimenting different pathologies, CVD for instance, and thus it is fundamental to reduce time spent above the glycemic target range. Thanks to *Algorithm 4*, the statistics regarding the TAR are heavily improved with respect to DUAL I. In fact, this is the only metric which shows a statistical difference with DUAL I at the sixth month. There is a significant reduction at 1 month, in fact *Algorithm 4* provides a median TAR of 54%, while DUAL I shows a median of 62%. Moving to the third month evaluation, the statistical difference is preserved, as well as for a marked reduction of the TAR metric (Algorithm 4 TAR = 41%, DUAL I TAR = 51%). When considering the sixth month the TAR difference is reduced, this is because (the same goes for the TIR) DUAL I has enough time to reach high dosages that

normalize the subject glycemia. As a consequence, there is the absence of statistical difference at nine and twelve months. However, for all the time considered, and especially for the sixth, nineth and twelfth month, the IQR provided by the *Algorithm 4* are much lower than those associated to DUAL I. The benefits of IQR reduction are already described for the TIR.
Finally, looking at the FPG, a statistical difference is observed within the first month of the trial showing a reduction in the FPG, thus, the *Algorithm 4* median FPG is 134 mg/dL while for DUAL I is 156 mg/dL. However, the FPG value evaluated at the third month of the in-silico trial is almost the same and considering the sixth, nineth and twelfth month assessment the median FPG of *Algorithm 4* tends to be higher. Nevertheless, there are not statistical differences with the DUAL I ones. Moreover, despite the first and third month, considering the sixth, the nineth and twelfth month the IQR provided by the *Algorithm 4* are higher.
Tables 3.11, 3.12, 3.13, 3.14 and 3.15 show the numeric value of the metrics and the p-values of the statistical tests.

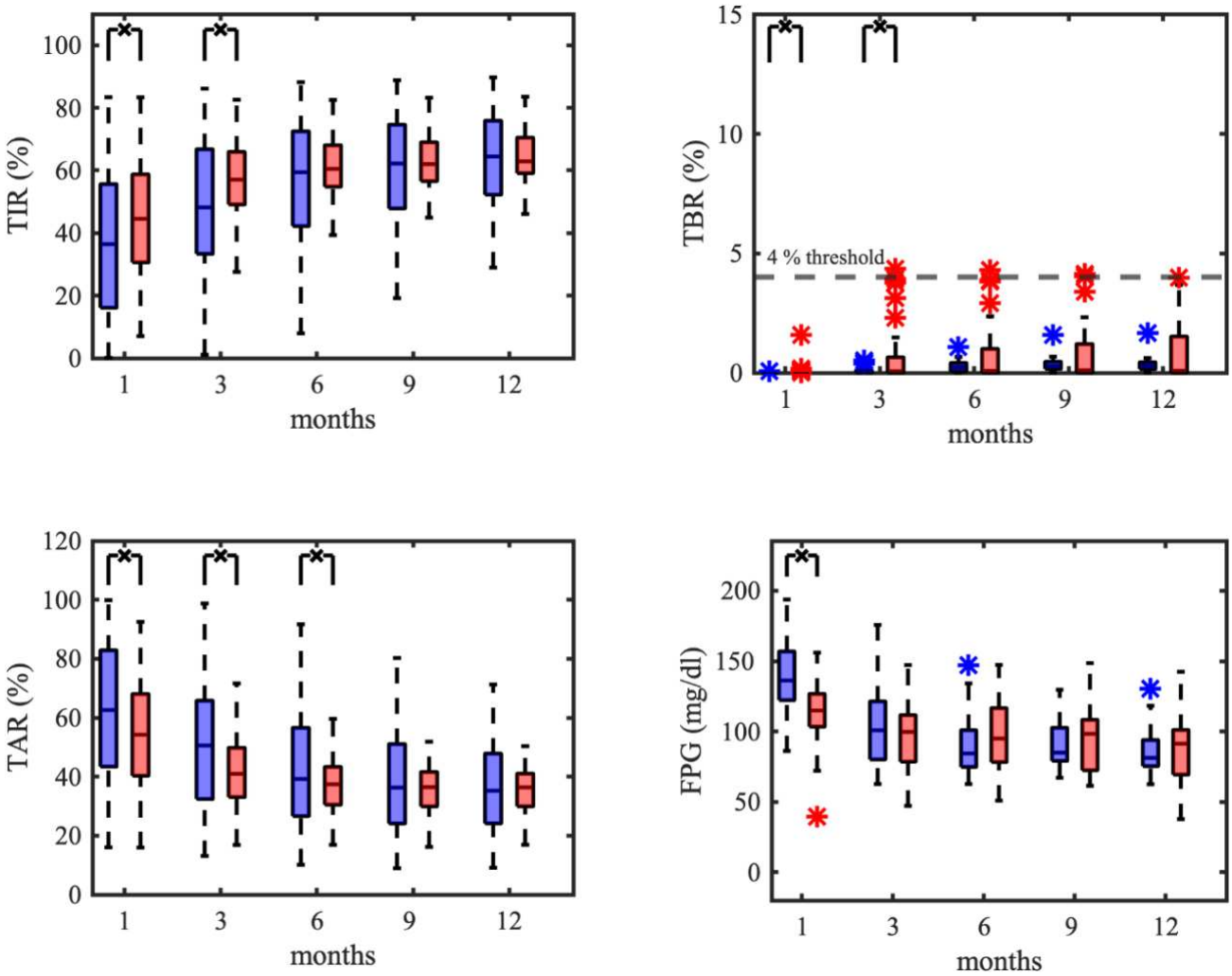

Figure 3.4 CGM-metrics and FPG after 1st, 3rd, 6th, 9th and 12th months for DUAL I (blue) and Algorithm 4 (red). In the upper left panel the TIR result are showed, in the upper right panel the TBR results are presented, while in the lower left panel the TAR results are showed and in the lower right panel there are the FPG results. Statistical differences are marked by black crosse

TIR (%) comparison					
Time	1st month	3rd month	6th month	9th month	12th months
Algorithm 4	44.55[28.10]	57.07[16.75]	60.51[13.18]	61.98[12.35]	62.90[11.24]
DUAL I	36.42[39.43]	48.20[33.36]	59.39[30.23]	62.18[26.74]	62.18[23.64]
p-value	$\mathbf{2.78 * 10^{-8}}$	$\mathbf{4.25 * 10^{-5}}$	0,05	0.31	0.55

Table 4 TIR (median [IQR]) comparison at different time points between Algorithm 4 (first line) and DUAL I (second line). Bold p-values (third line) represent statistical differences between the two rules according to Mann-Whitney test.

TAR (%) comparison					
Time	1st month	3rd month	6th month	9th month	12th months
Algorithm 4	54.19[27.64]	41.00[16.67]	37.42[12.79]	36.41[11.63]	36.35[11.06]
DUAL I	62.59[39.41]	50.58[33.36]	39.19[29.91]	36.30[26.91]	35.20[23.69]
p-value	$\mathbf{2.78 * 10^{-8}}$	$\mathbf{3.27 * 10^{-5}}$	**0.04**	0.20	0.42

Table 3.12 TAR (median [IQR]) comparison at different time points between Algorithm 4 (first line) and DUAL I (second line). Bold p-values (third line) represent statistical differences between the two rules according to Mann-Whitney test)

TBR (%) comparison					
Time	1st month	3rd month	6th month	9th month	12th months
Algorithm 4	0[0]	0.06[0.65]	0.08[1.00]	0.11[1.2]	0.08[1.51]
DUAL I	0[0]	0[0.11]	0.23[0.34]	0.28[0.30]	0.27[0.28]
p-value	**0.01**	$\mathbf{2.20 * 10^{-3}}$	0.17	0.13	0.11

Table 3.13 TBR (median [IQR]) comparison at different time points between Algorithm 4 (first line) and DUAL I (second line). Bold p-values (third line) represent statistical differences between the two rules according to Mann-Whitney test)

FPG (mg/dL) comparison					
Time	1st month	3rd month	6th month	9th month	12th months
Algorithm 4	134.81[23.26]	119.70[32.95]	114.92[38.16]	118.32[35.78]	111.34[31.65]
DUAL I	156.16[34.59]	120.77[41.15]	104.37[26.02]	104.86[23.54]	101.25[18.48]
p-value	**0.01**	$\mathbf{2.20 * 10^{-3}}$	0.17	0.13	0.11

Table 3.14 FPG (median [IQR]) comparison at different time points between Algorithm 4 (first line) and DUAL I (second line). Bold p-values (third line) represent statistical differences between the two rules according to Mann-Whitney test)

As mentioned in this thesis, one of the strengths of the novel CGM approaches is the possibility to provide a faster titration to patients. This can be seen in the average track of the FPG computed using the HIN population, as well as for the HIN population mean dose (figure 3.5). As one can see in the lower panel of the figure 3.5, the *Algorithm 4* provides, on average, a steep descend of the FPG and brings this metric to values comparable to the ones achieved by DUAL I in about 60 days, while DUAL I takes about 130 days to do the same job. Thus, the novel approach can provide faster lowering of the FPG, bringing the subject to be less exposed to the risks related to hyperglycemia. However, since the FPG is not considered in the *Algorithm 4*, the FPG SD is higher than the one associated to DUAL I.

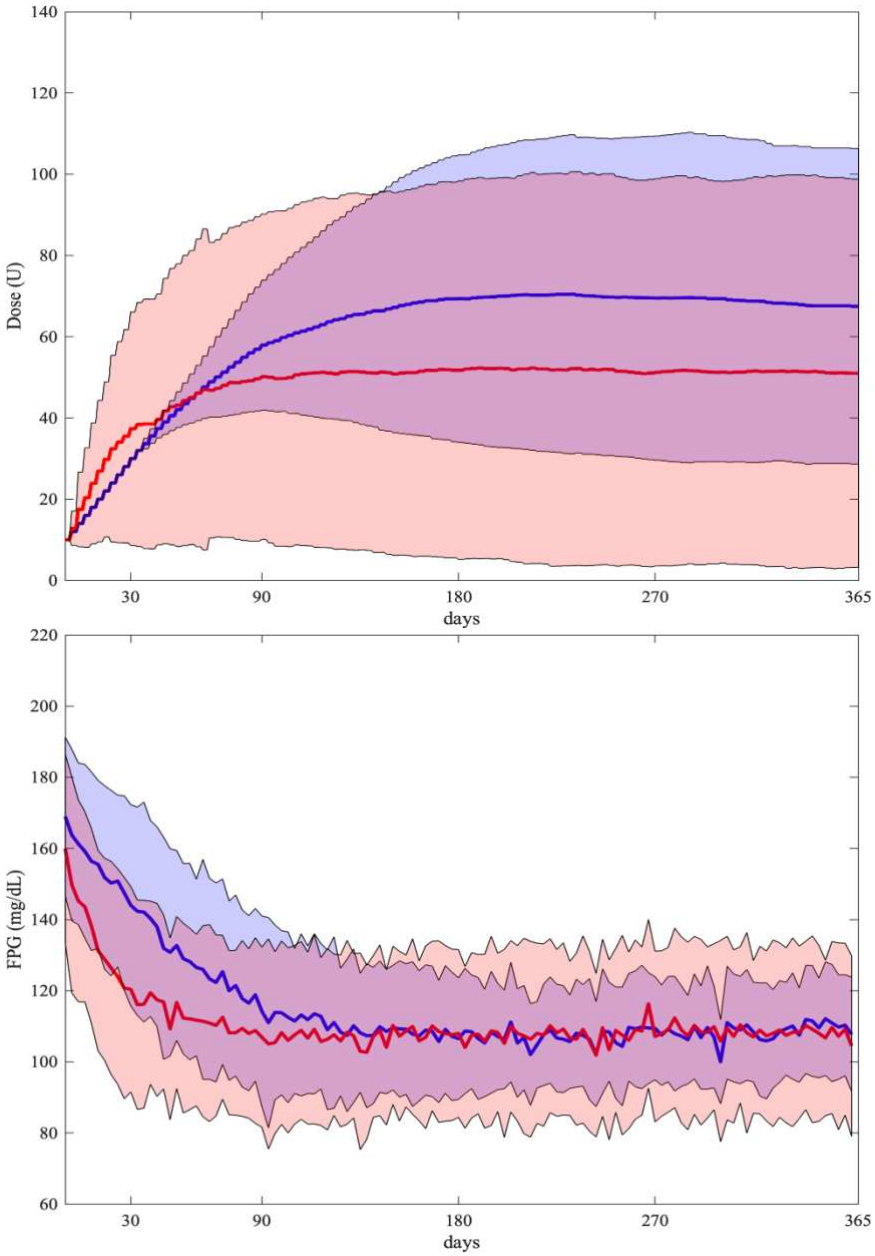

Figure 3.5 In the upper panel the mean±SD dose of Algorithm 4 (blue line and area) and of DUAL I dose (red line and area) are showed. In the lower panel the average HIN population FPG is presented.

The FPG results showed that the statistical differences are limited to the first months of the trial. This occurs because the insulin needs of T2D patients do not change when changing the titration rule, hence the final dose needed by subjects remains the same. What changes is the velocity at which the patients arrive to the optimal dose and the criteria that it should satisfy. When considering the velocity, as showed by the table 3.10, the mean convergence time (i.e., when the optimal insulin dose is found) of the *Algorithm 4* is located way before of the one achieved by DUAL I. For this reason, it is interesting to assess possible statistical differences which can occur when comparing the metrics computed until the mean time at which the *Algorithm 4* starts to administer its optimal dose, i.e. 61 days. Since this is a new cumulative time checkpoint the normality test were performed again, to understand which statistical test use. In the table 3.15 the Shapiro-Wilk test results are showed for the mean convergence time.

Algorithm ***4***		***DUAL I***	
Time Metric	*61 Days*	*Time Metric*	*61 Days*
TIR	0.81	*TIR*	0.19
TAR	0.40	*TAR*	0.20
TBR	$7.55 * 10^{-9}$	*TBR*	$3.34 * 10^{-11}$
FPG	0.68	*FPG*	0.57

Table 3.15 Algorithm 4 and DUALI Pvalues of the Shapiro-Wilk test

This shows the possibility for the TIR, the TAR and the FPG of using the paired t-student test instead of the Mann-Whitney test, since both *Algorithm 4* and DUAL I, provides normal distributed metrics according to the Shapiro-Wilk test.

In figure 3.6, a graphical representation of the results is showed. It is confirmed what said for the previous analysis, by applying the new Algorithm for the first 61 days of the in-silico trial, statistical differences are found in all the metric. Confirming the better performances of the *Algorithm 4* for the TIR, the TAR and the FPG. However, at 61 days the differences are confirmed by a more powerful test such as the t-test. Although, there is also a statistical difference in the median of TBR, which indicates that there is a significant shift in the median when using *Algorithm 4* of $5.7 * 10^{-3}$ %, which is quite small and not clinically significant. In table 3.16, the mean/median with the relative SD/IQR are reported for the *Algorithm 4* and DUAL I.

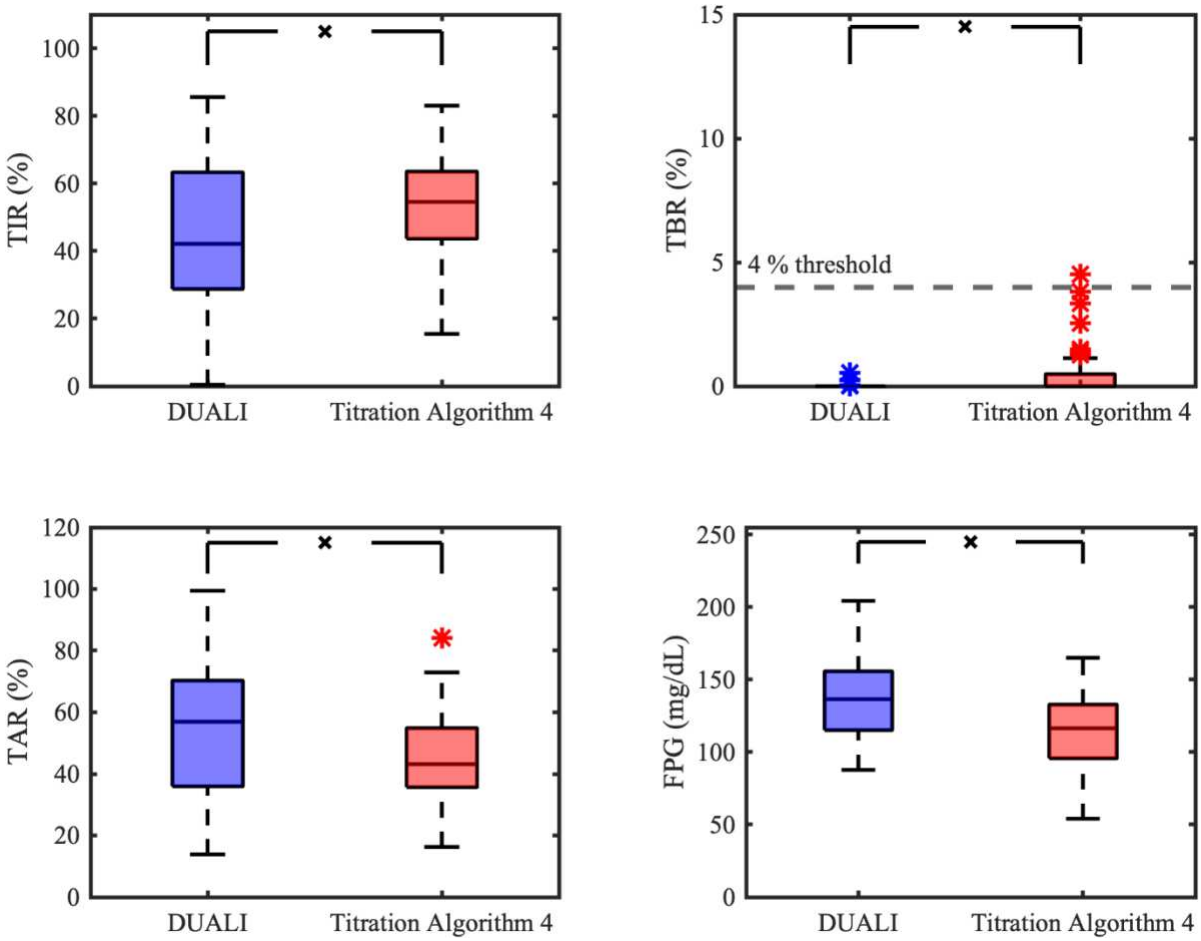

Figure 3.6 Shows the results at 61 days (i.e., the mean time at which Algorithm 4 administer its optimal dose) for DUAL I (blue) and Algorithm 4 (red). In the upper left panel, the TIR result are showed, in the upper right panel the TBR results are presented, while in the lower left panel the TAR results are showed and in the lower right panel there are the FPG results. Statistical differences are marked by black crosses.

CGM-metrics comparison at convergence time				
Time	TIR (%)	TBR (%)	TAR (%)	FPG (mg/dL)
Algorithm 4	55.53±13.99	$5.7\ 10^{-3}$ [0.48]	45.02±13.97	113.98±27.72
DUAL I	42.55±22.32	0 [0]	56.51±22.43	138.26±27.30
Pvalues	**$3.98\ 10^{-7}$ (#)**	**$2.32\ 10^{-4}$ ($)**	**$3.03\ 10^{-7}$ (#)**	**$8.80\ 10^{-4}$ (#)**

Table 3.16 61-days comparison between Algorithm 4 (first line) and DUAL I (second line). TIR, TBR, TAR and FPG are reported as median [IQR] if not normally distributed, mean±SD instead. Bold p-values (third line) represent statistical differences between the two rules according to Student-T test (#) or Mann-Whitney test ($).

CHAPTER 4

Conclusion

This thesis presented a novel CGM based basal-insulin titration rule for type 2 diabetes. First, the common back bone of each Algorithm was presented to the reader, followed by the part describing how to compute the CGM long-term trend and extracting relevant features from it (i.e., the mean slope of the curve), as well as the computation of the CGM metrics (TIR, TAR, TBR and, FPG). In fact, they can be used as a solid information for up-titrating patients to their optimal basal-insulin dose, rather than using just average three-days FPG, which is used by the state-of-the-art method, i.e. DUAL I rule.

Then, the four different version of the Algorithm implemented were outlined. Each one is characterized by different improvements, which corrected one or more undesired behaviors that can occur with the previous version. In fact, the first version of the Algorithm had the tendency to provide doses that brings the patient to periodic hypoglycemic event, even severe. The following versions avoided this way of acting thanks to the implementation of a specific flag, coupled with a dedicated system for saving the previous administered doses.

Another pitfall was the prefixed 10 U increment. Thus, the next step was to implement a proportional increment system based on some subject information. The solution was found by considering an increment related to the minimal clinically significant TIR improvement (i.e., a 5% variation), thus, an increment that provides relevant clinically benefits to the subject. Moreover, the information needed came from the current and the previous iteration: the correspondent TIR values were evaluated within a cartesian plane to find the dose increment that satisfies the up mentioned criterion.

Lastly, the fourth version was focused on improving the behavior before the convergence to the optimal insulin dose is reached, using a smoother and less aggressive dosing scheme.

Another important step was understanding which Algorithm had the best performances. In the first place each version was compared one with the others by using an appropriate version of the ANOVA test: there were no statistical differences between the new proposed Algorithms, however one can appreciate the improvements done for some of the outliers in the TBR as well for the TAR. Therefore, the best algorithm was picked considering the Pearson correlation calculated between the final optimal doses administered by DUAL I and the ones administered by each version of the algorithm. *Algorithm 4* was picked as the best algorithm given it provides the highest correlation coefficient (ρ=0.82) with DUAL I. Thus, the results between the last version of the Algorithm and DUAL I are discussed in this work.

At the beginning, when considering the comparison between the best algorithm and DUAL I, five different cumulative time check points were considered: 1 month, 3 months, 6 months, 9 months, and 12 months. For all the CGM metrics, differences were found for the first- and third-month cumulative time checkpoints. Moreover, for the TAR the statistical median difference was preserved also for the sixth month checkpoint. This is expected because, ideally, the dose needed by the subject does not depend on the specific titration rule used, but only on the time needed to reach the optimal insulin dosage. Thus, one of the main points of strength of the new approaches is the velocity of the titration process. Looking at the table 14, one can immediately see that the best algorithm has a mean convergence time of 61 days, versus the 151 days needed by DUAL I. The benefits are obvious, if a patient is up-titrated faster he will sake of an improved glycemia, which is reflected by better CGM

time metrics and FPG. To support the importance of administering faster titration rule, another cumulative time checkpoint was considered: the mean convergence time of the *Algorithm 4*; as expected, the TIR, the TAR and the FPG were improved to the respect of DUAL I.
On the other hand, there are some drawbacks of administering a more aggressive basal-insulin titration rule. First, as discussed in this thesis, it makes sense to apply such rules only in subject that needs them, thus, in those in which the insulin need is higher. However, when considering the *Algorithm 4* applied to the HIN population statistical differences were found in TBR at the first-, third-month cumulative time checkpoints, as well as at the *Algorithm 4* mean convergence time. This is a natural consequence of a faster titration. In fact, it is expected that reaching the target faster using higher dose increments, the probability of providing to the subject a dose which is over the optimal one is higher. Practically, this was reflected in slightly higher values of the TBR metric. However, these differences were found only in the first and third month of the trial, and even in those time checkpoint the median differences were low (i.e., 0.06% TBR variation when applying the *Algorithm 4* titration). Moreover, at the sixth-, the nineth- and the twelfth-month checkpoint differences are not found anymore, and all the *Algorithm 4* outliers are below the 4% threshold defined by the international consensus. Resulting that the safety of the T2D Algorithm user is not compromised.
It is important to underly that when considering the HIN population, the *Algorithm 4* provide an almost doubled clinically significant improvement of the TIR and the TAR within the first 3 months, bringing a risk reduction of hyper-glycemia related complications. Moreover, insulin-naïve T2D subjects experiment an improvement of the quality of life, deriving from a more effective and efficient glycemic control. Finally, the first month and the sixty-first day FPG are significantly reduced even if this metric is not considered into the implementation of *Algorithm 4*.
However, further improvements to the proposed method can be made. In fact, the trend analysis of the CGM signal proved to be a powerful tool for controlling the glycemia of T2D subject. It provided information which can be used for the implementation of new basal insulin titration rule which are faster and more effective. For this reason, future improvement concerns the aggressiveness of the *Algorithm 4*. In fact, studies that aims to better tune the aggressiveness of the titration rule can be carried out to provide a more general rule, thus, not limited to HIN patients. Furthermore, considering a titration rule with an optimized aggressiveness, it could be associated to a lower probability of administering too high doses, resulting in an improved TBR, which is the only pitfalls of the *Algorithm 4* when comparing it to DUAL I. Moreover, another future improvement can be the usage of the other trends (ST and R) to achieve even a better glycemic control with respect to the one obtained with *Algorithm 4*. Sticking to the LT trend improvements, future study can focus on extracting more than one feature, also coming from other domains (i.e., frequency). Finally, all the extracted features could be unified into an index, which can be used within the decision-making process in order to better understand the subject glycemic status.

1. Khan, M. A. B. *et al.* Epidemiology of Type 2 Diabetes – Global Burden of Disease and Forecasted Trends. *J. Epidemiol. Glob. Health* **10**, 107–111 (2020).

2. Galicia-Garcia, U. *et al.* Pathophysiology of Type 2 Diabetes Mellitus. *Int. J. Mol. Sci.* **21**, 6275 (2020).

3. Mokdad, A. H. *et al.* Prevalence of Obesity, Diabetes, and Obesity-Related Health Risk Factors, 2001. *JAMA* **289**, 76–79 (2003).

4. Riddy, D. M., Delerive, P., Summers, R. J., Sexton, P. M. & Langmead, C. J. G Protein–Coupled Receptors Targeting Insulin Resistance, Obesity, and Type 2 Diabetes Mellitus. *Pharmacol. Rev.* **70**, 39–67 (2018).

5. Goodpaster, B. H., Kelley, D. E., Wing, R. R., Meier, A. & Thaete, F. L. Effects of weight loss on regional fat distribution and insulin sensitivity in obesity. *Diabetes* **48**, 839–847 (1999).

6. Coppelli, A. & Prato, S. D. TRATTAMENTO DEL DIABETE DI TIPO 2.

7. Insulin Basics | ADA. https://diabetes.org/healthy-living/medication-treatments/insulin-other-injectables/insulin-basics.

8. Bruttomesso, D. *et al.* Restoration of early rise in plasma insulin levels improves the glucose tolerance of type 2 diabetic patients. *Diabetes* **48**, 99–105 (1999).

9. Heise, T., Nosek, L., Bøttcher, S. G., Hastrup, H. & Haahr, H. Ultra-long-acting insulin degludec has a flat and stable glucose-lowering effect in type 2 diabetes. *Diabetes Obes. Metab.* **14**, 944–950 (2012).

10. Wang, W. *et al.* DUAL I China: Improved glycemic control with IDegLira versus its individual components in a randomized trial with Chinese participants with type 2 diabetes uncontrolled on oral antidiabetic drugs. *J. Diabetes* **14**, 401–413 (2022).

11. Zinman, B. *et al.* Insulin degludec versus insulin glargine in insulin-naive patients with type 2 diabetes: a 1-year, randomized, treat-to-target trial (BEGIN Once Long). *Diabetes Care* **35**, 2464–2471 (2012).

12. American Diabetes Association. 8. Pharmacologic Approaches to Glycemic Treatment: Standards of Medical Care in Diabetes-2018. *Diabetes Care* **41**, S73–S85 (2018).

13. Bruen, D., Delaney, C., Florea, L. & Diamond, D. Glucose Sensing for Diabetes Monitoring: Recent Developments. *Sensors* **17**, 1866 (2017).

14. Wang, J. Real-Time Electrochemical Monitoring: Toward Green Analytical Chemistry. *Acc. Chem. Res.* **35**, 811–816 (2002).

15. Zafar, H., Channa, A., Jeoti, V. & Stojanović, G. M. Comprehensive Review on Wearable Sweat-Glucose Sensors for Continuous Glucose Monitoring. *Sensors* **22**, 638 (2022).

16. Battelino, T. *et al.* Clinical Targets for Continuous Glucose Monitoring Data Interpretation: Recommendations From the International Consensus on Time in Range. *Diabetes Care* **42**, 1593–1603 (2019).

17. Goodarzi, M., Sharma, S., Ramon, H. & Saeys, W. Multivariate calibration of NIR spectroscopic sensors for continuous glucose monitoring. *TrAC Trends Anal. Chem.* **67**, 147–158 (2015).

18. American Diabetes Association. 6. Glycemic Targets: Standards of Medical Care in Diabetes-2020. *Diabetes Care* **43**, S66–S76 (2020).

19. Lu, J. *et al.* Association of Time in Range, as Assessed by Continuous Glucose Monitoring, With Diabetic Retinopathy in Type 2 Diabetes. *Diabetes Care* **41**, 2370–2376 (2018).

20. Beck, R. W. *et al.* Validation of Time in Range as an Outcome Measure for Diabetes Clinical Trials. *Diabetes Care* **42**, 400–405 (2019).

21. Beck, R. W. *et al.* The Relationships Between Time in Range, Hyperglycemia Metrics, and HbA1c. *J. Diabetes Sci. Technol.* **13**, 614–626 (2019).

22. Vigersky, R. A. & McMahon, C. The Relationship of Hemoglobin A1C to Time-in-Range in Patients with Diabetes. *Diabetes Technol. Ther.* **21**, 81–85 (2019).

23. Klonoff, D. C. ADAG Study Group Data Links A1C Levels with Empirically Measured Blood Glucose Values - New Treatment Guidelines Will Now be Needed. *J. Diabetes Sci. Technol.* **8**, 439–443 (2014).

24. Visentin, R., Schiavon, M. & Dalla Man, C. In Silico Cloning of Target Type 2 Diabetes Population for Treatments Development and Decision Support *. in vol. 2020 5111–5114 (2020).

25. Holst, J. J. *et al.* IDegLira Improves Both Fasting and Postprandial Glucose Control as Demonstrated Using Continuous Glucose Monitoring and a Standardized Meal Test. *J. Diabetes Sci. Technol.* **10**, 389–397 (2015).

26. Bonet, J., Visentin, R., Vettoretti, M., Facchinetti, A. & Man, C. D. Smart Titration of Long-Acting Insulin in Insulin-Naïve Type 2 Diabetic Subjects. (2023).

27. Gorzalczany, S. B. & Rodriguez Basso, A. G. Strategies to apply 3Rs in preclinical testing. *Pharmacol. Res. Perspect.* **9**, e00863 (2021).

28. Visentin, R., Cobelli, C. & Dalla Man, C. The Padova Type 2 Diabetes Simulator from Triple-Tracer Single-Meal Studies: In Silico Trials Also Possible in Rare but Not-So-Rare Individuals. *Diabetes Technol. Ther.* **22**, 892–903 (2020).

29. Dalla Man, C., Rizza, R. A. & Cobelli, C. Meal simulation model of the glucose-insulin system. *IEEE Trans. Biomed. Eng.* **54**, 1740–1749 (2007).

30. Piccinini, F., Dalla Man, C., Vella, A. & Cobelli, C. A Model for the Estimation of Hepatic Insulin Extraction After a Meal. *IEEE Trans. Biomed. Eng.* **63**, 1925–1932 (2016).

31. Eaton, R. P., Allen, R. C., Schade, D. S., Erickson, K. M. & Standefer, J. Prehepatic insulin production in man: kinetic analysis using peripheral connecting peptide behavior. *J. Clin. Endocrinol. Metab.* **51**, 520–528 (1980).

32. Schiavon, M. *et al.* In Silico Head-to-Head Comparison of Insulin Glargine 300 U/mL and Insulin Degludec 100 U/mL in Type 1 Diabetes. *Diabetes Technol. Ther.* **22**, 553–561 (2020).

33. Sherwin, R. S. *et al.* A model of the kinetics of insulin in man. *J. Clin. Invest.* **53**, 1481–1492 (1974).

34. Kahn, B. B. & Flier, J. S. Obesity and insulin resistance. *J. Clin. Invest.* **106**, 473–481 (2000).

35. Zhigljavsky, N. G., Vladimir Nekrutkin, Anatoly A. *Analysis of Time Series Structure: SSA and Related Techniques*. (Chapman and Hall/CRC, 2001). doi:10.1201/9780367801687.

36. Hassani, H. A Brief Introduction to Singular Spectrum Analysis.

37. Aas, K. & Haff, I. H. The Generalized Hyperbolic Skew Student's t-Distribution. *J. Financ. Econom.* **4**, 275–309 (2006).

38. Kalra, S. *et al.* Hypoglycemia: The neglected complication. *Indian J. Endocrinol. Metab.* **17**, 819–834 (2013).

39. Shapiro, S. S. & Wilk, M. B. An Analysis of Variance Test for Normality (Complete Samples). *Biometrika* **52**, 591–611 (1965).

40. Kim, T. K. T test as a parametric statistic. *Korean J. Anesthesiol.* **68**, 540–546 (2015).

41. Mann, H. B. & Whitney, D. R. On a Test of Whether one of Two Random Variables is Stochastically Larger than the Other. *Ann. Math. Stat.* **18**, 50–60 (1947).

42. Kruskal, W. H. & Wallis, W. A. Use of Ranks in One-Criterion Variance Analysis. *J. Am. Stat. Assoc.* **47**, 583–621 (1952).